Investigation of acoustic whole blood plasmapheresis for minimization of endogenous blood loss in neonatal care

Tobias Lindgren

2021

Master's thesis in

Biomedical Engineering

Main supervisor: Andreas Lenshof

Co-supervisor: Thomas Laurell

LUND UNIVERSITY

Faculty of Engineering, LTH

Department of Biomedical Engineering

Abstract

Early erythrocyte transfusion is common in infants born extremely premature. Research has shown that these children are at greater risk of morbidity later in life, and that iatrogenic blood loss from blood sample analysis is one of the contributing factors to the need for transfusions.

Acoustophoresis-based plasmapheresis could potentially be used to reduce the loss of endogenous blood components through return of erythrocytes to the bloodstream. The aim of this thesis was to provide a proof of concept for the use of peristaltic pumps in acoustophoresis-based whole blood plasmapheresis.

An experimental acoustic separation setup with peristaltic pumps was constructed and used to extract plasma from whole blood. Functionality of the peristaltic pumps were evaluated based on separation performance measured with flow cytometry.

Measurements showed that the pulsations generated by peristaltic pumps have a large negative effect on functionality of acoustic separation. However, the combination of peristaltic pumps with pulsation dampers were shown to greatly improve performance and achieved separation equivalent to when syringe pumps were used. The result of this thesis supports the use of peristaltic pumps in acoustophoresis-based plasmapheresis with whole blood.

Keywords: Acoustophoresis, microfluidics, peristaltic pump, flow cytometry, plasmapheresis, whole blood, extremely premature infants.

Preface

This master thesis was performed during the period of February to September, 2021 at the department of Biomedical Engineering at Lund University. The thesis work was supervised by main supervisor Andreas Lenshof and assistant supervisor Thomas Laurell. Examinator of this master thesis was Per Augustsson.

Acknowledgement

First, I would like to express my gratitude to my supervisors, Andreas Lenshof and Thomas Laurell, for guiding me through this thesis and providing with everything that was needed. Secondly, I want to thank Axel Tojo, for taking the time to help me with 3D printing. I also want to thank everyone in the lab who helped me and who made me feel welcome.

Table of Contents

ABSTRACT ..... **III**

PREFACE ..... **V**

ACKNOWLEDGEMENT ..... **VII**

INTRODUCTION **1**

1.1 PROBLEMS 3
1.2 PURPOSE, AIM & GOAL 4
1.3 DISPOSITION 4

THEORY **5**

2.1 BLOOD 5
2.1.1 Blood based diagnostics *7*
2.1.2 Blood transfusion *7*
2.2 MICROFLUIDICS 8
2.3 ACOUSTOPHORESIS 11
2.3.1 Primary acoustic radiation force *12*
2.3.2 Acoustic streaming *13*
2.3.3 Shear induced diffusion *13*
2.4 FLOW CYTOMETRY 13
2.5 MICROFLUIDIC FLOW CONTROL 14

MATERIALS & METHOD **15**

3.1 EXPERIMENTAL SETUP 15
3.2 ACOUSTIC SEPARATION OF POLYSTYRENE BEADS 19
3.3 ACOUSTIC SEPARATION OF WHOLE BLOOD 19
3.3.1 Pulsation damper *19*
3.3.2 Sampling loop *20*
3.4 ANALYSIS OF SEPARATED BLOOD FRACTIONS 21
3.4.1 Gating strategy *21*

RESULTS & DISCUSSION **23**

4.1 THE EXPERIMENTAL SETUP 23
4.1.1 Measure of pump volume flow rate *23*
4.1.2 The acoustic separator *24*
4.1.3 The peristaltic micropump *26*
4.1.4 The pulsation damper *27*
4.1.5 Sampling loop *32*
4.1.6 Analysis of flow cytometry data *34*
4.2 SEPARATION AND FUNCTION 36
4.2.1 Separation with polystyrene beads *36*
4.2.2 Separation with whole blood *36*
4.2.3 Acoustic separation with fetal blood *41*

CONCLUSION **43**

REFERENCES **44**

List of figures & tables

- Figure 1: The experimental setup from above. Visible parts in the image are (1) the inlets and the outlets of the acoustic separator, (2) the piezoceramic transducer, (3) the two peristaltic micropumps, and (4) the input sample container. 15
- Figure 2: Images of (a) the acoustophoresis chip that was initially used and (b) the second chip that was used. 16
- Figure 3: Illustration of different pump configurations.....17
- Figure 4: Images shows (a) the PDMS pump head membrane with the Ω-shaped microchannel visible in the center and (b) the complete pump with (1) the pump membrane, (2) the pump rollers, and (3) the rotary motor. Images taken from the pump manufacturers webpage, (Chip Pump - ACP-29/QCP-29 - Takasago Fluidic Systems (takasago-fluidics.com)). 18
- Figure 5: Homemade pulsation dampers.....20
- Figure 6:Illustration of the sampling loops two positions, fill and flush..21
- Figure 7: Flow cytometry data from whole blood which was used for placement of gates around identified cell populations. 22
- Figure 8: Flow cytometry data from sample with stained cells. Used to identify cell populations in FSC vs SSC plot. 22
- Figure 9: Measure of the volume flow rate for both pumps using both membrane sizes. 23
- Figure 10: Image sequence (a-f) with deposits released from the walls of the separation channel and trapped in the flow splitter 25
- Figure 11: Whole blood separation (a) with pulsation damper and (b) without pulsation damper. 27
- Figure 12: Comparison of separation with syringe pumps and peristaltic pumps. All separations were performed on the same day with whole blood from the same donor and each measure was performed only once. The measured red cell concentration also contains white blood cells, however, the fraction of white cells account for less than 1% of the total blood volume and therefore have minimal contribution to the measured concentration. 28
- Figure 13: Separation when using (a) peristaltic pumps with pulsation dampers (b) syringe pumps at a side flow rate of 8 μl/min. 29

- Figure 14: Low frequency pulse when using pulsation damper. (a) Pulse start, red cells are diverted to the side branches. (b) Direction of diverted flowlines are returned to the center outlet. (c) Flow returning to a stable state after the pulse ends.....30
- Figure 15: Red/white cell concentration different side flow rates in plasma separated using the two different types of home-made pulsation dampers. 31
- Figure 16: Red/white cell concentration in samples collected from the sample loop (blue) and the pump connected to the side outlet (red).....34
- Figure 17: Flow cytometry data in three different samples collected from side outlet (**a-c**) and center outlet (**d-f**) when using pulsation dampers. The flow rate in center outlet was 58 µl/min and the flow rate in side outlet was (**a, d**) 10.55 µl/min (**b,e**) 14.95 µl/min (**c, f**) 19.36 µl/min.....35
- Figure 18: Pulsation generated by the peristaltic pumps. (a) Start of a new pulsation, beads are directed from the center of the channel into the side branches. (b) End of the pulsation, beads stay in the center and follow the flow into the center outlet.....36
- Figure 19: Overview of separated blood fractions. 37
- Figure 20: Comparison of red/white cell concentration in plasma using different side flow rates with and without a pulsation damper. 38
- Figure 21:Comparison of platelet concentration in plasma using different side flow rates with and without pulsation damper. 39
- Figure 22: Red/white cell concentration in both outlets from separation with pulsation damper using different flow rates for each pair. The same whole blood sample was used for all three pairs. 40
- Figure 23: Red/white cell concentration in both outlets from separation with pulsation damper using different flow rates for each pair. Concentration of the whole blood sample that was used for all three pairs is also included. 41

List of acronyms & abbreviations

NICU(s) = Neonatal intensive care unit(s)

GA = Gestational age

Hb = Hemoglobin

HbF = Fetal hemoglobin

HbA = Adult hemoglobin

VLBW = Very low birthweight (<1500 g)

RBCT = Red blood cell transfusion

BPD = Bronchopulmonary dysplasia

ROP = Retinopathy of prematurity

POC = Point-of-care

LOC = Lab-on-a-chip

RBC = Red blood cell

HCT = Hematocrit

ID = Inner diameter

OD = Outer diameter

PDMS = Polydimethylsiloxane

PS = Polystyrene

FSC = Forward scatter

SSC = Side scatter

FACS = Fluorescence-activated cell sorting

PBS = Phosphate-buffered saline

PerCP = Peridinin chlorophyll protein complex

APC = Allophycocyanin

SID = Shear induced diffusion

To the love of my life, Karin

Chapter 1

Introduction

Survival and viability threshold of extremely premature infants have steadily been increasing during recent decades. In Sweden, the 1-year survival of premature babies, born between 22-26 gestational weeks, increased from 70% in 2004-2007 to 77% in 2014-2016.[1]. The progress in Sweden is believed to be largely due to centralization and standardization of the routine for neonatal advanced life support in combination with active care from both caretakers and parents. Tocolytic treatment, antenatal corticosteroids, and surfactant treatment within 2 hours after birth[2], has been associated with reduced risk of infant death[3].

In Sweden, approximately one tenth of all newly born infants require medical care and start their life in a neonatal intensive care unit (NICU). One third of these children are born preterm, meaning they are born before 37 weeks of pregnancy. The period between conception and birth is referred to as gestation and the term gestational age (GA) is commonly used to describe how far along a pregnancy is. Based on GA, newborns can be classified as either preterm (< 37 weeks), full term (37-42 weeks), or post-term (> 42 weeks). Preterm births are further divided into the subgroups, late preterm (32-37 weeks), very preterm (28-32 weeks), and extremely preterm (< 28 weeks). Although survival of extremely preterm babies has increased, the risk of morbidity later in life is still high and inversely increases with GA[4].

The development and maturation of many vital organs occurs during the last weeks and months of pregnancy. Human lungs go through five different stages of development during fetal life. It is not until the end of the third stage, the canalicular stage (16-26 weeks), that the lungs are sufficiently developed to support independent life[5]. The potential surface area for gas exchange is at this point very small and does not rapidly increase until after 30 gestational weeks. Extremely premature babies are most often in need of respiratory assistance as well as constant observation of both pulse and breathing.

The immune system in premature babies is also not fully developed. Making them extra sensitive and susceptible to infections. Health of infants in the NICU is therefore constantly being supervised through various diagnostics tests. Blood plasma and whole blood samples are needed to measure blood gases, blood chemicals, and hematologic status[6]. Which requires frequent daily blood sampling. The most used method to obtain cell-free blood plasma is through centrifugation of whole blood, in which the remaining blood components are discarded after separation[7].

1. Introduction

All newborns undergo a physiological decline in hemoglobin (Hb) concentration. This is a natural part of the transition from a hypoxic intrauterine environment to an oxygen rich extrauterine environment. The decline is the result of different physiological changes with one of the biggest contributing factors being the transition from the high oxygen-affinity fetal hemoglobin (HbF) to lower oxygen-affinity adult hemoglobin (HbA)[8].

The blood volume of newborns is approximately 80 mL/kg[9]. Extremely preterm infants with very low birth weight (VLBW) can weigh as little as 500 grams. The combination of a very small blood volume and many weeks of intensive care with frequent blood sampling results in large laboratory blood losses relative to body weight. The heavy iatrogenic blood loss further reduces hemoglobin concentration and results in varying degrees of anemia and need for red blood cell transfusion (RBCT). Frequent diagnostic assessment has been found to be a primary cause of anemia in extremely preterm infants[10]. The total laboratory blood loss of infants in the NICU varies greatly with GA, birth weight, and place of treatment. A study on Swedish babies born before 30 gestational weeks, published by Hellström et al.[11], found the average laboratory blood loss relative to body weight during the first two weeks to be 42 mL/kg (52% of total blood volume).

The adult blood used for RBCTs of infants with anemia, so called “top-ups”, have a different blood composition compared to fetal blood. This includes hemoglobin, stem cells, steroids, and growth factors[4],[9]. For extremely preterm infants or VLBW infants the transferred blood volume is strongly correlated to the total laboratory blood loss[12],[13]. Potentially exceeding 100% of the total blood volume during the first two postnatal weeks[11],[14].

Replacing large portions of the endogenous fetal blood with adult blood during the first weeks of postnatal life has been shown to increase the risk of morbidity later in life. Especially the development of bronchopulmonary dysplasia (BPD)[4],[11] and retinopathy of prematurity (ROP)[14]. However, the full effect on development and growth is still not fully understood.

Reducing the need for early RBCT is of interest both medically to improve life of premature infants and economically to reduce the cost of healthcare. Important steps have been made in the progress of developing effective blood conservation techniques and strategies that will help reduce the likelihood of anemia of prematurity. Most effective and promising are optimization of circulatory blood volume at birth, maintaining optimal nutrition, and minimizing blood loss from laboratory testing. This can be achieved through development of minimal sampling techniques and point-of-care (POC) diagnostics[9], [10],[15].

Research and development of POC diagnostics have greatly increased during recent years. In part due to advancements in microtechnology techniques and

through development of microfluidic lab-on-a-chip (LOC) devices[16]. LOCs are small integrated devices that can perform several laboratory functions on the same platform. The combination of microfluidics and biosensors in LOCs improves the possibility to develop easy-to-use portable devices that can perform all the conventional laboratory functions in real-time using less sample volume, ideal for POC diagnostics[17].

One problem, common to both POC diagnostics and diagnostic blood loss of premature babies, is the preparation of blood plasma for analysis. Blood plasma is widely used in clinical diagnostics because it contains many biomarkers that can be used to indicate changes related to various diseases[18]. Centrifugation of whole blood is the classical and most widely used method to obtain cell-free plasma. The centrifuge method is a time and labor-intensive batch-process that constitutes a problem for development of POC diagnostics[19].

Separation of blood plasma is also a major contributing factor to the large loss of endogenous blood components associated with laboratory testing of premature infants[4]. This is because blood plasma makes up about 55% of the blood's various constituents and after separation by centrifugation the remaining 45% of the blood is discarded, including the high Hb red blood cells, white blood cells and platelets. The solution to this problem requires development of new methods for plasma separation that reduce blood loss and can be integrated in POC diagnostic devices.

Processes and methods for generating plasma that include returning blood after the plasma has been separated and removed are called plasmapheresis. The focus of this thesis is a new concept method for acoustic plasmapheresis to minimize loss of endogenous blood components. Acoustophoresis-based separation to generate cell-free plasma from whole blood has been previously used and integrated in a microfluidic platform for the detection of prostate cancer biomarkers[7, 18]. The idea is to use an acoustophoresis-based separation chip to continuously extract cell-free plasma from whole blood in a closed system that returns the enriched blood cell fraction to the patient.

1.1 Problems

For plasmapheresis of preterm infants to be possible, it is crucial that the returning blood fraction is not contaminated. The problem with previously mentioned acoustophoresis-based devices[18] is the use of syringe pumps to drive the flow through the microfluidic chip. Syringe pumps operate in a batch wise manner which is problematic for both continuous separation and minimizing risk of contamination. Plasma extraction of infants in closed controllable environments, such as incubators, need to be possible without exposure to the outside environment, for which the bulky aspect of syringe pumps constitutes a problem[20].

The advantage with syringe pumps is that they generate a very steady flow with high controllability, ideal for acoustophoresis-based separation that require a steady laminar flow for high separation efficiency. For this application however, another type of pump is needed, one that can generate a continuous steady flow without risk for contamination.

Peristaltic pumps are a type of pump that are more common in medical applications. Especially when risk of contamination needs to be minimal and continuous flow during long periods is needed. The disadvantage of these pumps, in terms of separation with acoustophoresis, is the generation of a pulsating flow.

In this thesis, the use of peristaltic pumps for acoustophoresis-based plasma separation is investigated. An experimental setup with two peristaltic micropumps is constructed and plasma is extracted from whole blood. The effect of pulsatile flow on separation and methods to reduce pulsations are also investigated and tested.

1.2 Purpose, aim & goal

The purpose for this thesis is to provide a "proof of concept" for the use of peristaltic pumps in acoustophoresis-based whole blood plasmapheresis. The aim is to investigate the concept by construction of an experimental setup with peristaltic micropumps and generate cell-free plasma from whole blood with acoustophoresis. The goal is to provide a foundation for future research and development of acoustophoresis-based POC-devices that reduce loss of endogenous blood components to help improve the life of premature infants.

The aims of this thesis are to:

- Build an experimental setup for acoustophoresis-based separation with peristaltic micropumps.
- Evaluate the performance of said pumps.
- Perform continuous extraction of cell-free plasma from whole blood.
- Investigate the concept of returning blood in a closed system.

1.3 Disposition

This report consists of five chapters. Chapter one introduces the background and purpose of this study. Chapter two discusses the underlying theory of this thesis. Chapter three describes the method used to obtain the results, as well as the development of the experimental setup during the study. The results of the study are discussed in chapter four. Finally, Chapter five presents the conclusion of the thesis.

Chapter 2

Theory

In this chapter, the first section covers some of the basics of blood and its components as well as blood-based diagnostics and blood transfusion. The second section includes microfluidics, acoustophoresis, flow cytometry, and microfluidic flow control.

2.1 Blood

Blood is a complex non-Newtonian fluid involved in transport of oxygen and nutrients, removal of carbon dioxide and waste products, maintenance of hemostasis, temperature regulation, defense, and cell signaling[21]. Human blood consists of a collection of specialized blood cells including erythrocytes (red blood cells), leukocytes (white blood cells), and thrombocytes (platelets), suspended in a liquid matrix called plasma.

Red blood cells (RBC)

RBCs are the most abundant of all blood cells. RBC are highly deformable cells without nucleus, approximately 7.8 μm in diameter, and shaped like biconcave disks[22]. For adults, all RBCs are produced in the bone marrow of certain bones and circulate the body for about 120 days before being broken down in the spleen and the liver[23].

The amount of red blood cells in human blood is usually measured in volume percent, called hematocrit (HCT). In adults, HCT is between 42-54% for men and 37-47% for women[22]. The volume of RBCs is approximately 90 fL and normal RBC count for adult blood is between 4-6 million cells per microliter[24].

The main function of RBCs is transportation of oxygen from the lungs to all the tissues of the body. Transport is mainly facilitated through hemoglobin, which is a protein with high oxygen affinity. For oxygen transport across the placenta to be effective, the baby's blood contains fetal hemoglobin, which has a higher affinity for oxygen compared to adult hemoglobin.

Reference intervals for HCT levels based on GA are used for premature infants instead of normal intervals as these have proven very difficult to determine. The reference value for GA between 29-34 weeks is 39-62% and for GA 35-42 weeks between 45-65%[25].

White blood cells (WBC)

The WBCs consist of various subtypes that all are part of the body's immune system and help in the defense against foreign pathogens. WBCs are generally classified based on presence of visible granules and morphology of their nucleus. Monocytes and lymphocytes belong to the group of mononuclear cells without visible granules. Granulocytes are granule-containing cells and consist of neutrophils, eosinophils, and basophils.

WBCs are much fewer in number than the RBCs and account for less than 1% of the total blood volume. Healthy adults have between 4500 and 11000 WBCs per microliter of blood[26]. The size of WBCs varies depending on subtype. From lymphocytes being the smallest and roughly the same size as RBCs to monocytes being the largest with diameters between 12-20 μm[27].

Differentiation of WBC subtypes is possible through expression of different surface markers within different groups. Common for all white blood cells is the expression of CD45, which is not present for RBCs or platelets.

Platelets

Platelets are small cell fragments without a nucleus. Approximately 2-4 μm in diameter and created by megakaryocytes in the bone marrow, they are responsible for blood clotting to prevent blood loss. Normal platelet count range between 150,000-400,000 per microliter[21].

Frequently used surface markers to identify platelets in whole blood include CD41 and CD42b, which are not present on other circulating blood cells[28].

Blood plasma

The blood plasma, derived when all blood cells are removed, is a straw-colored fluid consisting of 90-92 % water, 6-8 % proteins, and a mixture of other substances. Blood is made up of 55-60% plasma which main functions are to serve as the blood’s transport medium, maintain blood pressure, regulate temperature by distributing body heat, and maintaining pH balance[29]. Some of the constituents of plasma are amino acids, organic acids, vitamins, enzymes, hormones, dissolved gases, and electrolytes such as potassium, sodium, calcium, magnesium, and chloride. Majority of plasma proteins consist of three groups including albumin, globulins, and coagulation proteins[29].

2.1.1 Blood based diagnostics

Blood is a source of information for clinical healthcare and crucial for early detection and treatment of various diseases. Diagnostic blood samples can be used to monitor a person's health condition by identifying and following deviating test markers that indicate illness and evaluating and monitoring treatment response.

Some diagnostic tests can be performed using whole blood, while others require specific blood components to be removed or isolated. Different separation methods can be used depending on what component needs to be separated. Many of the biomarkers that are of interest for clinical blood diagnostics can be found in the blood plasma.

Centrifugation

A commonly used method for blood plasma separation is centrifugation. Tubes containing whole blood and anticoagulants are placed in a centrifuge and rotated at high speed. Blood cells are pushed outwards, towards the bottom of the tube, by the centrifugal force and packed in layers based on their size, shape, and density. RBCs are found at the bottom, followed by a layer containing WBCs and platelets commonly referred to as the buffy coat, and clean plasma is found at the top. Centrifugation of blood in a density medium allows for higher resolution in separation.

2.1.2 Blood transfusion

Blood transfusions can be directly lifesaving or the only way to stop a disease from rapidly progressing. However, it is important to weigh the benefits against the risks before transfusion with whole blood or any blood product is performed.

Red cell transfusion products

Benefits of RBC transfusion include increase in oxygen carrying capacity, improved tissue oxygenation, improved hemostasis, and improved coagulation. Some risks associated with RBC transfusion include serious hemolytic transfusion reactions, transfusion-related acute lung injury, transmission of infectious pathogens such as HIV, hepatitis B, hepatitis C, syphilis, and malaria. In addition to these risks, blood contamination from incorrectly handled is always possible.[30, 31]

Plasma transfusion products

Patients suffering from liver diseases or clotting factor deficiencies often need to receive plasma transfusion to avoid excessive bleeding from occurring. Plasma transfusions can also be beneficial to restore blood pressure, blood volume,

electrolyte levels, and prevent bleeding in the setting of coagulopathy or disseminated intravascular coagulation. Risks with transfusion of plasma products include transfusion reactions, including acute lung injury and circulatory overload, and the transmission of infections and pathogens that are present in whole blood. [32]

2.2 Microfluidics

Microfluidics involve studying the behavior and control of fluid constrained to the microscale. In the macro world, the behaviour of liquids is dominated by volume-based forces and the influence of the surface-based forces can often be neglected. When scaling down, volume decreases faster than surface area and on the micro scale, the dominating forces shift. Surface forces and viscosity instead decides the behavior of fluids, and some inertial forces such as gravity can often be neglected.

Laminar flow

Turbulence and mixing of flowlines decrease when scaling down into the micro domain. Here the laminar flows become more dominant, where particles move along smooth regular paths in parallel layers and the only mixing that occurs is governed by diffusion.

Newton's second law ($F = ma$) can be used to describe the motion of an object based on the center of mass motion. Instead of describing the motion of individual particles in a fluid, all particles can be treated as a continuum and motion can be described in terms of continuous fields with the Navier-Stokes equation. For an incompressible Newtonian fluid with density ρ, and dynamic viscosity η the equation is:

$$\rho\left[\frac{\partial u}{\partial t} + (u \times \nabla)u\right] = -\nabla p + \eta\nabla^2 u + f \quad (1)$$

For which p is pressure, u is velocity, t is time and f is an external acceleration field acting on the fluid body.

Reynolds number (Re) is a dimensionless number used for determining fluid flow conditions in microsystems. Re gives the ratio between magnitudes of inertial and viscous forces as:

$$Re = \frac{\rho d u}{\eta} \quad (2)$$

In which u is the average velocity of the fluid and d is the typical length scale (e.g. diameter, channel depth). Flows with $Re > 2300$ are considered turbulent and $Re < 2000$ are referred to as laminar[33]. Low Re and laminar flow can be obtained by reducing velocity, decreasing channel dimensions, or using fluids with higher viscosity.

Pressure driven flow

Solutions to the Navier-Stokes equation describe the flow for different sets of conditions. The solution for a pressure gradient driven flow through a capillary or channel is called Hagen-Poiseuille[33]. The volume flow, Q, is expressed as proportional to the pressure difference in a similar relation to that of Ohm's law for electricity ($V = RI$). For fluids the relation become:

$$Q = \frac{\Delta V}{t} = \frac{\Delta P}{R_h} \tag{3}$$

The hydraulic pressure, ΔP, is the pressure drop across the length of the channel or capillary. The hydrodynamic resistance, R_h, is dependent on channel geometry and fluidic viscosity, μ. In a channel of circular cross-section with radius r and length L, the resistance is:

$$R_h = \frac{8\mu L}{\pi r^4} \tag{4}$$

Pulsation damper

A pulsation damper can be used to stabilize pulsations in a pressure-driven flow generated from an oscillating pressure difference. The damper usually consists of a damper chamber filled with a gas that absorbs pressure variations by compressing and expanding. During compression, when the pressure is at its highest, the volume of the gas decreases and liquid is drawn into the chamber. As the pressure then decreases, the gas expands, forcing the liquid back into the system. In this way, part of the fluid pulse is stored in the damper and allowed back into the system between pulses.

For an ideal gas, the relation between pressure (p) and volume (v) is described by the ideal gas law as

$$pv = nRT \tag{5}$$

where n is the quantity of the gas in moles, T is the temperature, and R is the gas constant. For an isotherm process, follows from this relation that

$$p_1 V_1 = P_2 V_2 \tag{6}$$

in which p_1, v_1 and p_2, v_2 is the pressure and the volume of the gas before and after the process, respectively. For an isentropic process, in which there is no heat transfer to the surroundings, the same equation instead become

$$p_1 V_1^n = p_2 V_2^n \tag{7}$$

where n is a constant that is specific to the gas.

The behavior of a real gas deviates from that of an ideal gas, and the deviation is described by the compressibility factor Z which depend on both temperature and pressure as

$$\mathrm{Z} = \frac{pV}{nRT} \tag{8}$$

The compressibility factor can also be described as the actual molar volume of the gas compared to the calculated molar volume at the same temperature and pressure, $\mathrm{Z} = V_{real}/V_{ideal}$.

Flow profile

Pressure-driven flow of a fluid in a microchannels has a parabolic flow profile. Viscous drag against channel walls implies a no-slip boundary condition, leading to velocity being zero at the walls and increases towards the center. Particles will move at different velocities depending on distance to all the walls.

Stokes drag

Particles that are moved through a fluid by an external force experience a drag force opposite to the external force. The particles velocity will be accelerated by the external field until reaching terminal velocity. At this velocity the drag force, called Stokes drag, is equal to the external force and acceleration stops. Stokes drag (F_d) on a spherical particle of radius r, dynamic viscosity η, and velocity u is defined as

$$F_d = 6\pi\eta r u \tag{9}$$

Many of the external forces which cause movement, such as gravity and the primary acoustic radiation force, scales with particle volume. However, F_d scales with particle radius and therefore has a large impact on smaller particles. [34]

Particle sedimentation

Sedimentation of solid particles suspended in a fluid is a natural process due to the gravitational force and differences in density between the solids and the surrounding medium. Under the assumption of laminar flow, sedimentation of a spherical particle with radius r suspended in a liquid can be modeled by balancing the gravity force, the buoyancy force, and stokes drag force as

$$\frac{4}{3}\pi r^3(\rho_s - \rho_f)g = 6\pi\eta r u \tag{10}$$

where ρ_s and ρ_f is the density of the particle and surrounding fluid respectively, g is the acceleration of gravity, η is the viscosity of the fluid, and u is the velocity of the particle in the direction of gravity. When sedimentation velocity of the particle reaches terminal velocity (u_t), the gravity force is exactly balanced by the buoyancy force and the drag force. The particle will then fall through the fluid at a constant velocity. Solving equation (10) for terminal velocity yields the following expression for u_t

$$u_t = \frac{2}{9\mu} r^2(\rho_s - \rho_f)g \tag{11}$$

2.3 Acoustophoresis

Acoustophoresis refers to the resulting motion of a suspended particle from acoustic radiation forces when subjected to an ultrasound standing wave field. A primary radiation force, originating from scattering of the wave on the particle, causes the particle to move towards either a pressure node or antinode. Secondary acoustic radiation force, coming from interactions of scattered waves from two particles affects the relative particle-particle position.[35]

A standing wave is the result of interference from two waves travelling in opposite directions with the same amplitude and frequency. Acoustic standing waves are non-propagating, meaning that the location of pressure amplitude minima (pressure node) and pressure amplitude maxima (pressure antinode) is stationary. However, the amplitude of the standing wave at one point varies with time.

Acoustic separation is a continuous flow separation method in which ultrasound standing waves are formed in microchannels designed as resonance cavities. A half wavelength resonator is designed to form a standing wave with a single pressure node in the channel center and two pressure antinodes at the walls. Particles and cells can then be moved between different flow paths of a laminar flow and separated with a flow splitter. Acoustophoresis can be used for label-free

separation based on mechanical properties such as size, density, shape, and compressibility[36].

2.3.1 Primary acoustic radiation force

A simplified form of the primary radiation force from a one-dimensional standing wave, acting on a spherical particle with a radius a, much smaller than the sound wavelength λ, can be described by [37]

$$F_{rad} = 4\pi\Phi k a^3 E_{ac} \sin(2kz) \tag{12}$$

$$E_{ac} = \frac{p_a^2}{4\rho_o c_o^2} \tag{13}$$

$$k = 2\pi/\lambda \tag{14}$$

in which Φ is the acoustic contrast factor, z is particle position in the channel, p_a is the pressure amplitude, p_o and c_o are the density and speed of sound in the surrounding medium, and E_{ac} is the acoustic energy density which is proportional to the square of the voltage applied to the transducer.

The direction of the force on a particle is dependent on the acoustic contrast factor. Particles whose contrast factor is positive will migrate towards the pressure node, while particles with negative contrast factor will migrate towards the pressure antinode. The acoustic contrast factor is described by

$$\Phi = \frac{\kappa_o - \kappa_p}{3\kappa_o} + \frac{\rho_p - \rho_o}{2\rho_p + \rho_o} \tag{15}$$

where κ_o, ρ_o, κ_p, and ρ_p are the compressibility and density of the surrounding medium and particle, respectively. Particles moved by the primary acoustic radiation force will be affected by the earlier described Stokes' drag. The resulting velocity (u_{rad}) of the particle relative to the medium is described by

$$u_{rad} = \frac{2\Phi}{3\eta} a^2 k E_{ac} \sin(2kz) \tag{16}$$

in which η is the fluid viscosity. Particle velocity is dependent on the square of the radius. Separation of particles or cells which has the same physical properties is therefore size dependent.

2.3.2 Acoustic streaming

Streaming in the fluid is generated by the acoustic field due to shear stress near the walls. A half wavelength standing wave generates four acoustic streams which disturbs the laminar flow and induces Stokes drag on particles at the center of the channel. For microfluidic channels with resonance frequencies around 2 MHz large particles are dominated by the radiation forces and not moved by the streams, however, smaller particles that are less than $2\ \mu m$ are less affected by the acoustic radiation forces and instead follow the circular flow of streams[37].

2.3.3 Shear induced diffusion

Shear induced diffusion (SID) is the diffusive motion of particles in a shear flow due to hydrodynamical interactions between particles, induced by the relative velocity difference along streamlines [38]. The diffusion coefficient (D_s) for SID is

$$D_s = \dot{\gamma} R^2 f_s(\phi) \tag{17}$$

where $\dot{\gamma}$ is the local shear rate, R is the particle radius, and $f_s(\phi)$ is a function of the particle volume fraction ϕ. In an inhomogeneous suspension the particle flux (J_{SID}) can be expressed as

$$J_{SID} = -D_C(\phi)\nabla(\phi) \tag{18}$$

for which $D_C = \dot{\gamma} R^2 f_C(\phi)$ is the collective SID coefficient. SID is an anisotropic diffusion which increases with increasing particle concentration and scales to the power of the particle radius.

2.4 Flow cytometry

Microfluidics, optics, and electronics are combined in flow cytometry to create a powerful analyzing tool for rapid multiparametric analysis of particles and single cells in a solution[39]. In a traditional flow cytometer, the three systems are combined to analyze visible light scatter as well as fluorescence parameters.

The fluidic system consists of a flow chamber with a fast-flowing sheath fluid. Sample fluid is injected into the center of the sheath flow at a fixed volume flow rate which forms a two-layer laminar flow. Viscous forces between the layers increase sample flow rate, resulting in reduced cross-section area as the volume flow rate is fixed. The sample fluid is hydrodynamically focused into the interrogation point of a laser-based microscope. The optical system can consist of multiple lasers, with different excitation wavelengths, and collection optics in the form of steering filters and detectors that measure the intensity of different wavelengths. Detected light signals are converted by the electric system into

digital signals readable by a computer. The relative size and internal complexity of cells can be determined by measuring the forward scatter (FSC) and side scatter (SSC) respectively. Different fluorescent reagents such as fluorescently conjugated antibodies, DNA binding dyes, viability dyes and ion indicator dyes can further be used in flow cytometry to perform simultaneous characterization of mixed cell populations. [40]

2.5 Microfluidic flow control

Different microfluidic techniques can be used to generate and control flow in microfluidic systems. Common methods include use of pressure pumps, syringe pumps, and peristaltic pumps to generate flow.

Pressure pumps

A pressure pump can be used to control the pressure at different points of a microfluidic system. Applying pressure to the inlet fluid in a sealed container connected to the outlet generates a pressure driven flow. Pressure pumps are commonly used for applications that require high flow responsiveness, stability, and precision.

Peristaltic pumps

A peristaltic pump is a type of positive displacement pump which uses volume variations in a pump chamber to pressurize and move a fluid. Most peristaltic pumps generate flow through a rotary motion of rollers that compress a flexible tube or membrane, forcing the fluid inside to move. The rollers only compress the tube during part of each revolution. Between compressions the tube returns to its natural state, which draws fluid into the tube. This allows for fluid to be generated without the fluid being in direct contact with the pump's components, which is desirable for many medical applications. Peristaltic micropumps designed for easy integration in microfluidic systems are available and can generate very low flow rates with high precision during long time periods using a low voltage.

Syringe pumps

Syringe pumps are also a type of positive displacement pump and among the most used flow control systems for microfluidic systems. The volume inside a syringe is controlled through a mechanical system which moves the syringe piston and can be used to either push or draw fluid through a microfluidic system.

Chapter 3

Materials & Method

This chapter provides an overview and description of the experimental setup and its development throughout the project. This chapter also explains the methods and processes used to obtain the results of this study.

3.1 Experimental setup

Part of the project consisted of building the experimental setup for acoustophoresis-based separation (Figure 1). This was achieved by gradually adding components to solve various problems that appeared during the engineering process.

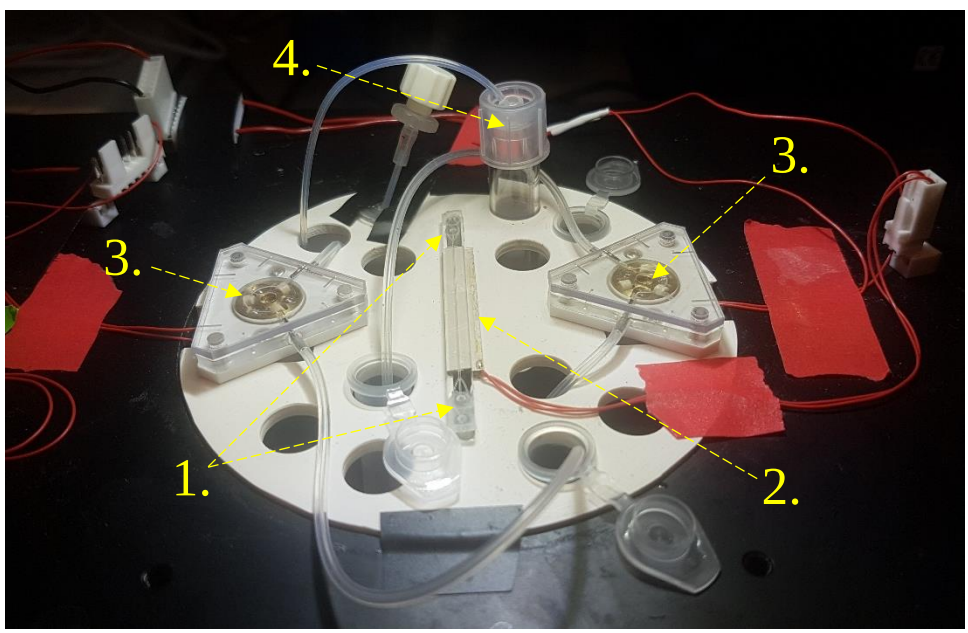

Figure 1: The experimental setup from above. Visible parts in the image are (1) the inlets and the outlets of the acoustic separator, (2) the piezoceramic transducer, (3) the two peristaltic micropumps, and (4) the input sample container.

The acoustic separator

A two-dimensional pre-alignment acoustophoresis chip was initially used, Figure 2(a). The chip was used without pre-aligning since it requires use of a buffer medium that would dilute and contaminate the blood. As the buffer inlet was plugged, this added unwanted dead volume where bubbles were prone to gather.

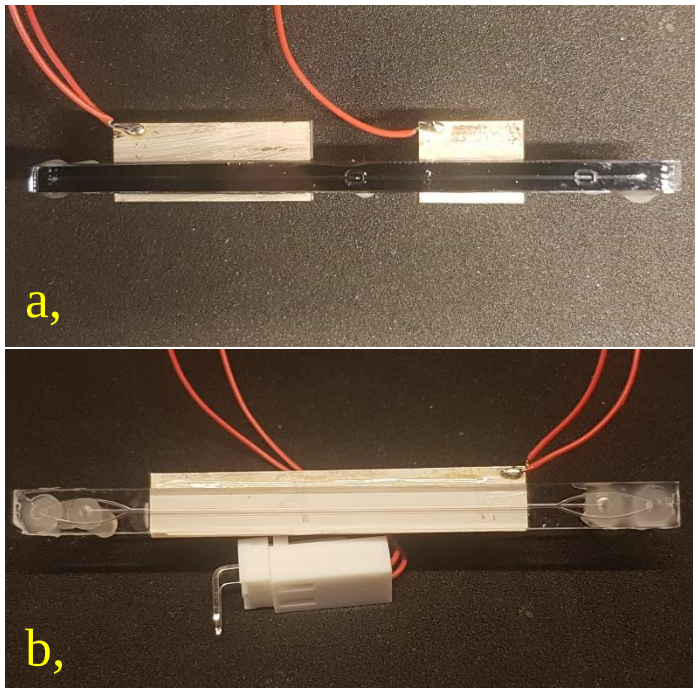

Figure 2: Images of (a) the acoustophoresis chip that was initially used and (b) the second chip that was used.

After initial testing the chip was replaced with another acoustophoresis chip, without pre-alignment and with softer corners at the flow splitter, Figure 2(b). The chip contains a straight separation channel with both ends symmetrically ending in a trifurcation with one central outlet/inlet and two side branches leading to the same side outlet/inlet. The central inlet was used as the sample inlet and the side inlet was used to purge the channel when clogged.

The separation channel is designed for a half-wavelength resonance frequency around 2 MHz, roughly 375 µm wide. A signal generator (Tektronix AFG 3022B) was used to actuate a piezoceramic transducer that was glued underneath the separation channel and generated the standing wave. Frequency and acoustic energy were monitored with an oscilloscope (Tektronix TDS 2002C) and separation was visually monitored with a camera (EO Edmond optics, EO 3112C) attached to a microscope.

The Peristaltic micropump

Flow through the experimental setup was generated with two peristaltic micropumps (Takasago ACP-29), for which three different pump configurations were tested (illustrated in Figure 3). In configuration A and B, blood input flow rate and one of the outlet flow rates are directly controlled by the pumps, while

the flow rate of the second outlet depends on the difference between the individual flowrates of the pumps. In configuration C, fluid is instead aspirated through the separation chip with pumps at both outlets, and blood input flow rate as the sum of the flow rates from both outlets.

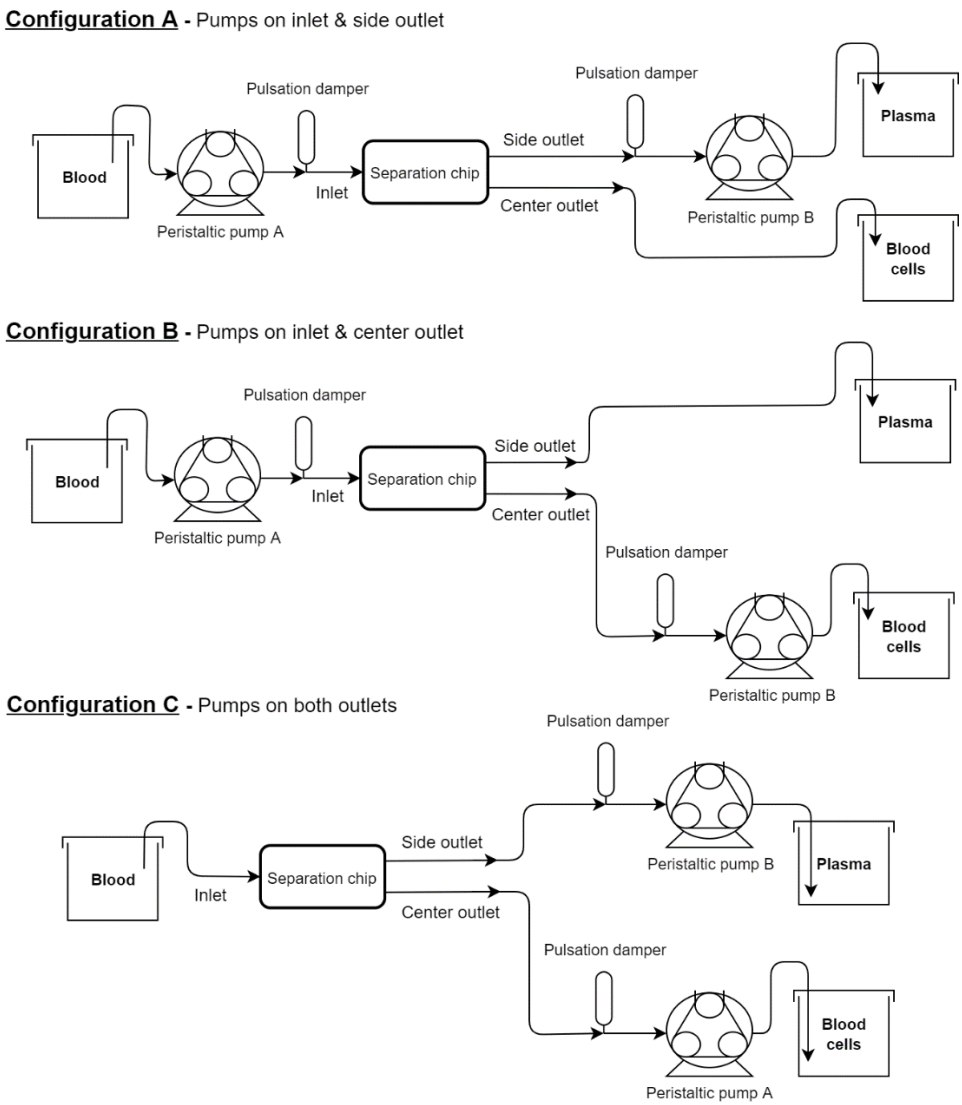

Figure 3: Illustration of different pump configurations.

Two power generators (Powerbox 3525 and Switchbox SB 15-20) were used to control and generate power to the pumps. The applied voltage was measured with a Fluke 75III multimeter during separation.

The pumps consist of three main parts. A Polydimethylsiloxane **(**PDMS) pump head membrane (Figure 4a) incorporating a Ω-shaped microchannel with pre-attached discharge/suction tubes, three pump rollers (Figure 4b), and a rotary motor (Figure 4b). The pump membrane, available with two different channel dimensions, is fixed on top of the pump rollers which then press against the elastic PDMS membrane blocking the microchannel and trapping fluid between the rollers. Trapped fluid is then pushed and moved by rotation of the rollers controlled by the applied voltage.

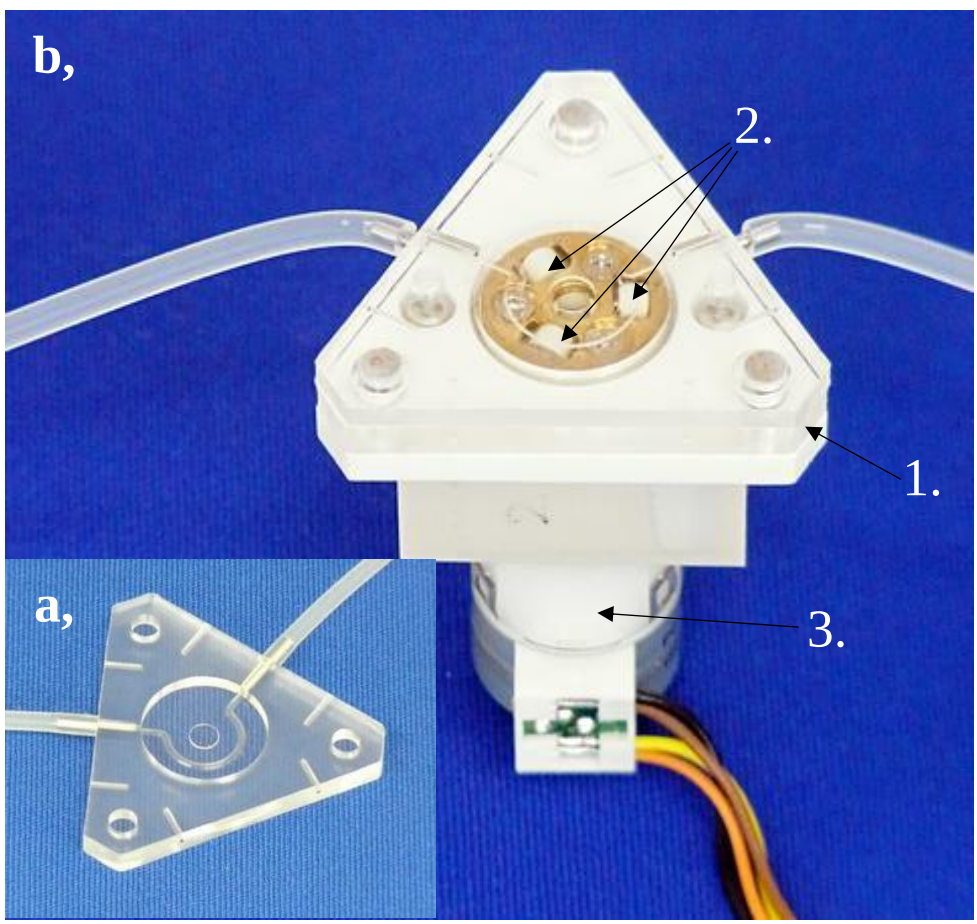

Figure 4: Images shows (a) the PDMS pump head membrane with the Ω-shaped microchannel visible in the center and (b) the complete pump with (1) the pump membrane, (2) the pump rollers, and (3) the rotary motor. Images taken from the pump manufacturers webpage, (Chip Pump - ACP-29/QCP-29 - Takasago Fluidic Systems (takasago-fluidics.com)).

3.2 Acoustic separation of polystyrene beads

Calibration of the experimental setup was visually performed using 5 µm and 7 µm polystyrene (PS) beads. Separation of PS beads suspended in ultrapure water (MilliQ) were performed using different pump configurations. Separation flow threshold was investigated through analysis of fluid collected from the side outlet using different flow rates.

3.3 Acoustic separation of whole blood

Whole blood from adult donors were collected in vacutainer blood collection tubes containing heparin (anticoagulant). The acoustophoresis chip was flushed with PBS to remove trapped bubbles before connecting the blood to the sample inlet. Influenced by the acoustic forces generated by the ultrasound transducer, operated at a frequency of 2.042 MHz and 9.5 V, blood cells migrated towards the channel center and clean plasma was generated at the side walls. Plasma fraction was extracted from the side outlet and enriched blood cell fraction was collected from the center outlet. Different flow rates of the pumps were used to investigate the effect on separation.

3.3.1 Pulsation damper

Pulsation dampers were used to reduce pulsations generated by the peristaltic pumps. The dampers consist of an air-filled damper chamber which acts as a compressible gas cushion that absorbs pressure differences. Two types of homemade dampers were used (Figure 5).

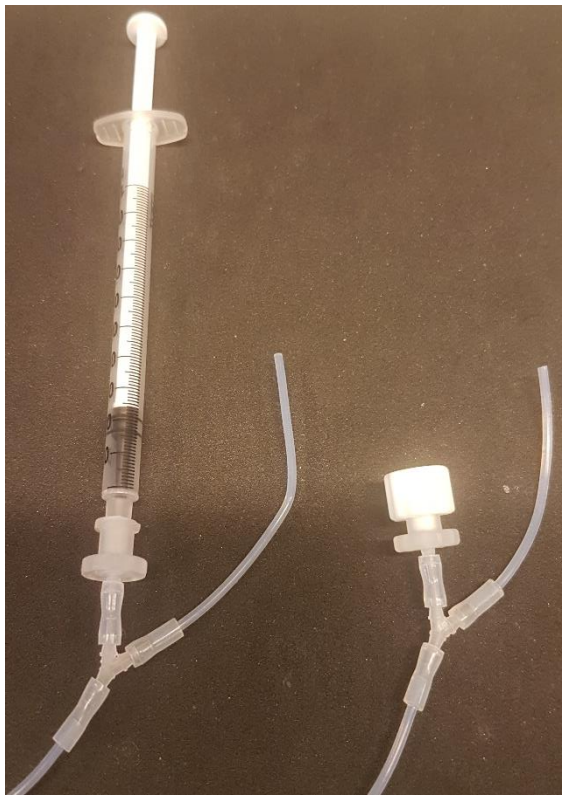

Figure 5: Homemade pulsation dampers.

These were both made from a microfluidic Y-connector with either a 1 ml plastic syringe or a plastic cap on one of the ends. Tubes connected the other two ends to the peristaltic pump and the microfluidic chip. Peristaltic pumps produce pressure spikes when operating that result in flow rate fluctuations. These can be reduced by the compression of gas in the damper chamber, resulting in a smoother flow.

3.3.2 Sampling loop

Fluid from the side outlet of the separation chip was collected in a 200 µl sampling loop. The loop consisted of a multiport with 6 ports and a 415 mm long tube (SUPELCO. TFE Teflon tubing) with an inner diameter (ID) of 0.8 mm. The multiport can be set in two positions, fill and flush, illustrated in Figure 6. When set to fill, fluid from the side outlet of the separation chip passes through the sampling loop before reaching the pulsation damper. When switching to flush, the sampling loop is bypassed and fluid flows directly to the pulsation damper. Air is then used to flush out and collect the fluid trapped in the loop. The loop was then cleaned and filled with PBS between each extraction of plasma.

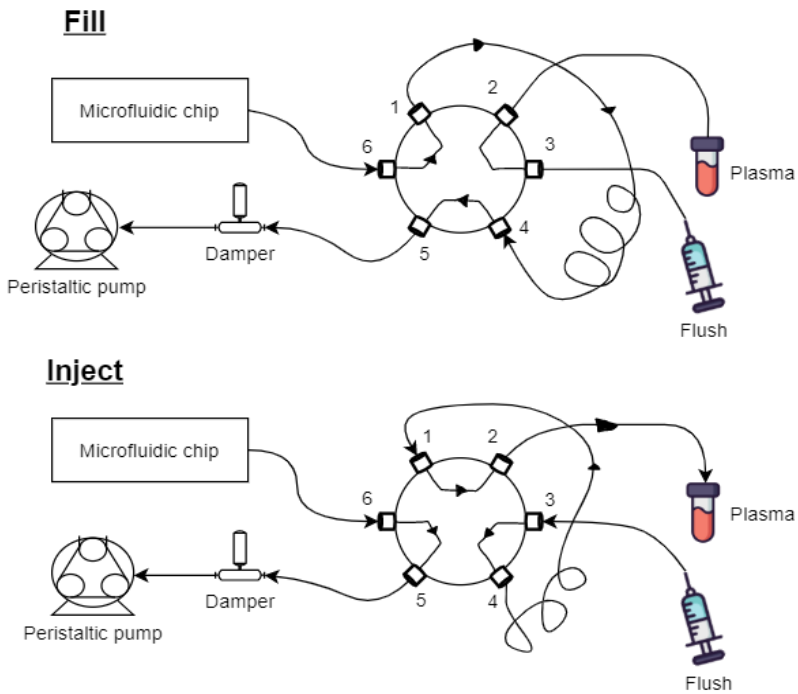

Figure 6:Illustration of the sampling loops two positions, fill and flush.

3.4 Analysis of separated blood fractions

Whole blood and separated blood fractions from the side and center outlet were analyzed with a FACS Canto II flow cytometer (BD Biosciences). Samples were diluted 1:1000 (side outlet) and 1:10000 (center outlet and whole blood) with PBS before analysis. Same flow cytometer setting was used for all samples, and medium injection flow rate (approximately 1 µl/sec) for a set time of 60 seconds.

3.4.1 Gating strategy

Monoclonal antibodies were added to some samples after separation to identify populations of WBC and platelets.

PerCP-conjugated antibodies towards CD45 and ACP-conjugated antibodies towards CD41a were used to identify leukocytes ($CD45^+$) and platelets ($CD41a^+$) in some samples (Figure 8). Fluorescence gates on PerCp and ACP signal allow the location of these two populations to be identified in a FSC vs SSC plot. With components, sizes, and relative amounts in blood being known, the conclusion was made that the unmarked cells found in the same population as leukocytes most likely are red blood cells. Gates placed around populations with platelet and red/white blood cells were used in analysis of all samples (Figure 7).

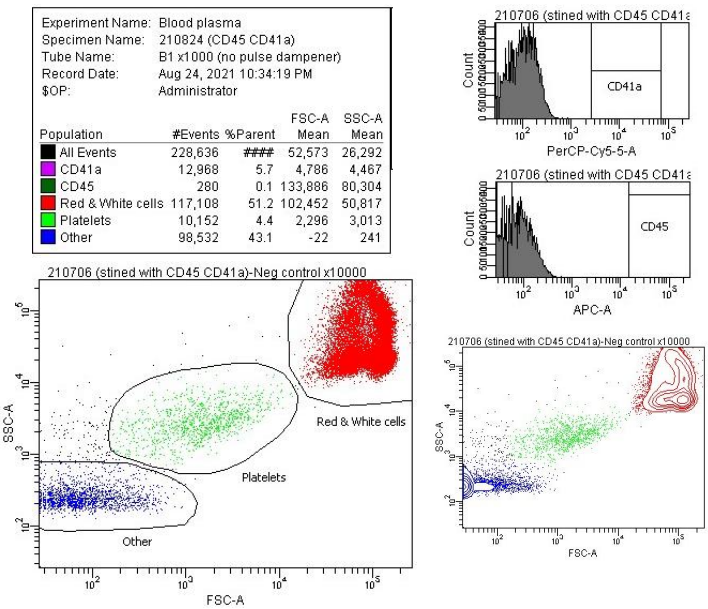

Figure 7: Flow cytometry data from whole blood which was used for placement of gates around identified cell populations.

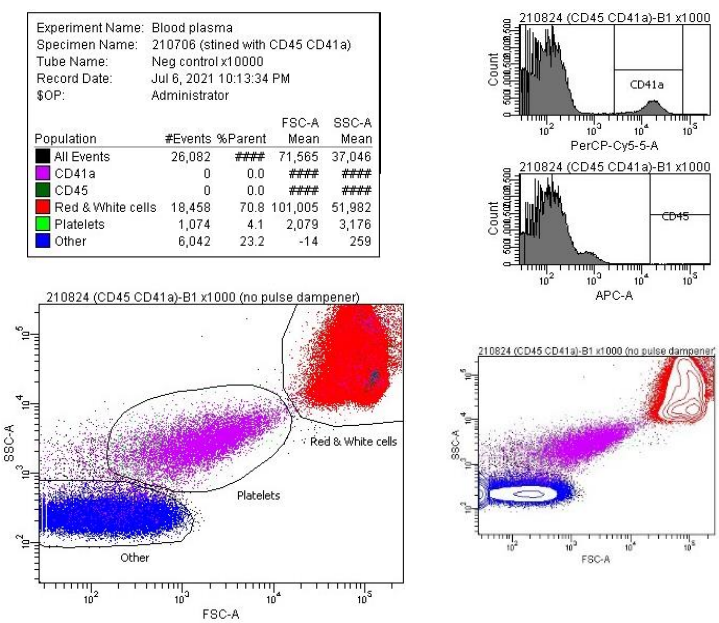

Figure 8: Flow cytometry data from sample with stained cells. Used to identify cell populations in FSC vs SSC plot.

Chapter 4

Results & discussion

4.1 The experimental setup

4.1.1 Measure of pump volume flow rate

Before investigating the effects on separation from peristaltic pumps, the volume flow rate from the pumps was measured. This was done by weighing MilliQ collected from the pump's outlet during a set time, Weight, density, and time was then used to calculate the volume flow rate using different applied voltages. Both pumps were measured using both available membrane sizes and showed similar time-averaged flow rate, which increases linearly with increased pump rotational speed (Figure 9). This correlates with the expected flow of volumetric pumps, for which the volume of pumped fluid in each cycle is identical. Pumping flow rate can therefore be linearly controlled by pump revolutions per minute (rpm)[41]. Volume flow rate also depends on the cross-section area of the pump membrane channel. For which only two different sizes were available during this project.

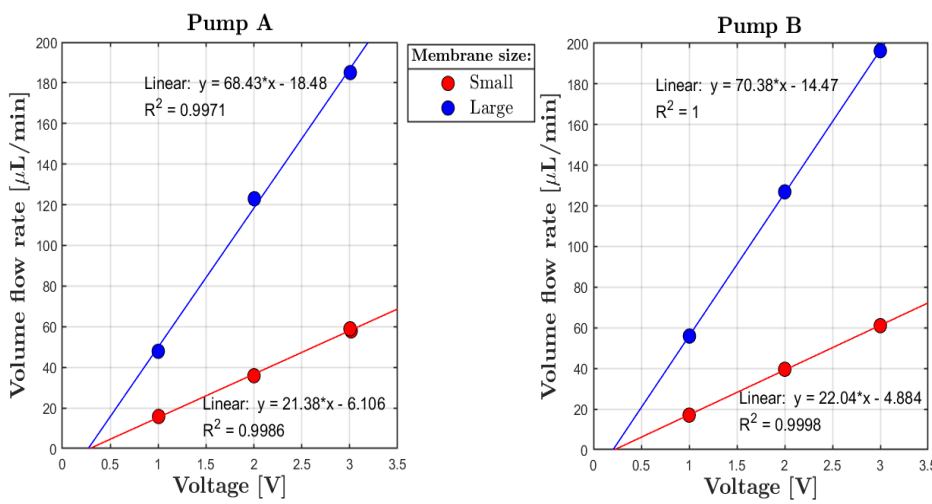

Figure 9: Measure of the volume flow rate for both pumps using both membrane sizes.

4.1.2 The acoustic separator

Regardless of whether a pulsation damper was used or not, a recurring problem was the presence of bubbles disrupting the flow. Bubbles that entered the separation channel would redirect red cells from the center into the side outlet and contaminate the attempt at gathering useful data. They constituted a constant threat to functionality and were the reason for many plasma extraction attempts having to be canceled or excluded from the results.

A common way for bubbles to form is through heterogenous nucleation. This is when dissolved gas molecules diffuse into tiny gas-filled pockets, such as cracks or irregularities in the channel walls. The result is the growth of bubble that eventually detach from the growing site and enters the system.

Changes in blood temperature may have contributed to the high incidence of bubbles during separation. The temperature of the blood changed from approximately 37 ℃ at the time of withdrawal, to 21 ℃ while being stored at room temperature, and then increased during separation due to heat generation from the ultrasound transducer. Gas solubility decreases with increasing temperature, lowering the amount of dissolved gas that the liquid can hold. This will in turn increase the rate of diffusion into gas pockets and the formation of bubbles.

Change in pressure also affect gas solubility and can influence the formation of bubbles. Henry's Law states that the amount of dissolved gas in a liquid is proportional to its partial pressure above the liquid, meaning that bubbles are more prone to form in liquids under low pressure.

It would have been interesting to investigate whether the presence of bubbles would have decreased if the blood had been kept at the same temperature as at the time of sampling. This could have been tested by having the test tube with blood in a hot water bath during the separation. Unfortunately, no thermometer was used in the experimental setup and the change in temperature of the blood due to heating by the ultrasound transducer is therefore unknown.

Bubbles were frequently observed to gather in the pump membrane channel. However, separation was not affected by these as the pumps were located downstream from the acoustic separator. Increased formation of bubbles in the membrane channel could be problematic for some applications and would need to be considered when designing acoustophoresis setups with peristaltic pumps.

With the peristaltic pumps not being able to create enough pressure to purge the system and remove the bubbles, a syringe had to be connected to the plugged inlet to flush PBS through the system. This serves a vital function, but also represents a potential problem for functionality that needs to be addressed.

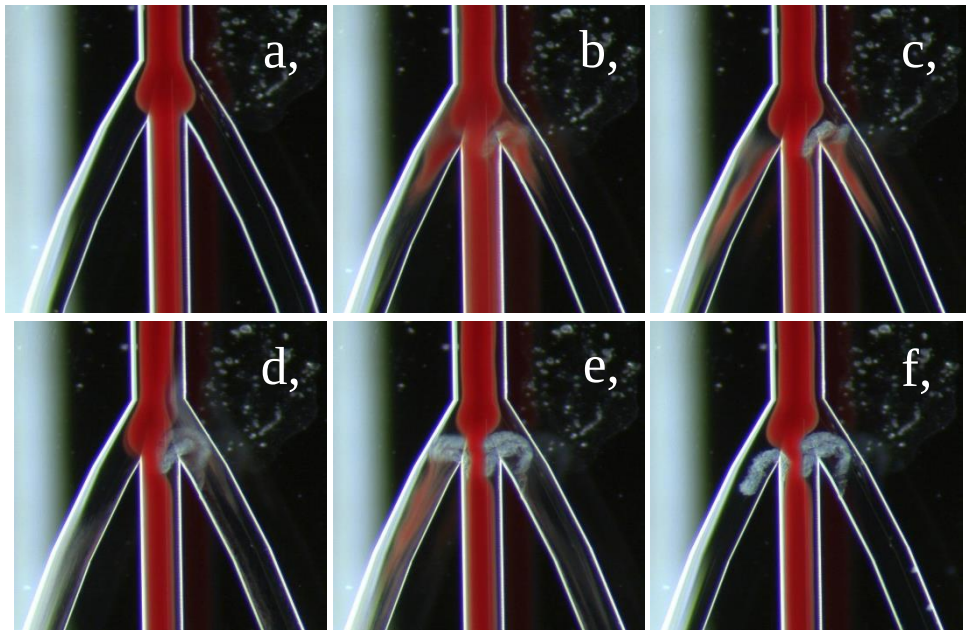

Figure 10: Image sequence (a-f) with deposits released from the walls of the separation channel and trapped in the flow splitter

With whole blood, it was observed that deposits accumulated in the antinodes along the walls of the separation channel. After growing large enough, the deposits detached from the walls and followed the flow, often ending up getting stuck in the flow splitter as shown by the image sequence in Figure 10.

These deposits are likely to be a combination of RBC hemolysis-activated platelets and intracellular components from broken cells. Separation attempts for which the system was filled with MilliQ water prior to separation showed increased formation of deposits and clogging of the system. The low concentration of ions in MilliQ water led to hemolysis of cells as water moves into the cells by osmosis and swelling of the cells can rupture the cell membrane, resulting in the leakage of cellular content. Release of Adenosine diphosphate (ADP) have been found to activate platelets and cell-free HB further enhance platelet activation by lowering the inhibitory effect of NO[42].

Separation stability and overall separation performance would likely be improved with an acoustophoresis chip that has been specifically designed for blood plasma separation of whole blood. Removing one of the inlets would decrease the dead volume of the system, which constitutes a potential site for bubble formation. Multiple outlets could be added along the bottom of the separation channel in a similar design used by Lenshof et al.[7] to sequentially remove red blood cells and

reduce RBC concentration at the flow splitter. Channel width at the location of these central outlets can also be increased to optimize removal of RBCs from these outlets as described by Karthick and Sen [43]. Placement of the piezoelectric transducer to the side of the separation chip instead of the bottom, have been suggested to improve transfer of acoustic energy and could further improve focusing of cells into the center of the channel.

A power amplifier was connected to the system which increased the acoustic energy to improve the focusing of cells. However, the focus of red cells did not improve markedly. Increasing the acoustic energy also increases the generation of heat, and can potentially overheat the acoustic chip, which can be harmful to cells, and affects speed of sound in blood. The resonance frequency of the microchannel depends on the speed of sound in the medium and temperature changes can therefore affect the formation of the standing wave. A temperature regulator could have been used to keep the temperature constant and allow higher acoustic energies to be used. Since the focus of this study was performance of peristaltic pumps, this led me to the decision to remove the amplifier and focus more on how pulsations could be reduced.

4.1.3 The peristaltic micropump

A heavy pulsatile flow was generated by the peristaltic pumps when pulsation dampers were not applied. Functionality of the acoustic separation was severely impaired independently of which pump configuration was used.

The separation performance of the different pump configurations was investigated with polystyrene beads. Based on visual observations, worst separation was found with the pumps on the inlet and the center outlet, configuration B. Separation was slightly improved with pumps on the inlet and side outlet, configuration A. Most stable flow was observed with the pumps placed at both outlets, configuration C. This is therefore the pump configuration preferred for separation with whole blood.

The flow profile of a peristaltic pump resembles that of a sawtooth function. With flow rapidly increasing until reaching a maximum and then almost instantly decreasing down to zero for a short period before rapidly increasing again. One of the problems for separation arises when the flow in the central outlet momentarily stops. The flow in the center of the channel is then for a short period diverted from the center outlet into the branches, resulting in contamination of RBCs in the side outlet. With the pumps positioned at the inlet and the side outlet, contamination of RBCs in the side outlet were mainly resulting from a short moment of backflow from the center outlet when the inlet flow was stopped by the pump.

A way to potentially reduce the negative effects on separation could be to have both pumps operating in phase at the same rpm. With the flow in both outlets starting and stopping in phase, flow of RBCs diverted into the wrong outlet could potentially be avoided. A potential problem with this approach is that the flow pulses would still not be in phase due to difference in flow resistance for the different flow paths. Mapping of the flow resistance for the whole system and simulations of the flow might be a good way to investigate this idea further. This approach also requires the pumps to be operating at the same rpm, for which they would have the same flow rates unless different membrane sizes were used. This was the main reason why creating new pump membranes was of interest. Unfortunately, this was not possible since the curing of PDMS did not work.

4.1.4 The pulsation damper

Visual observation of separation with pulsation damper showed that both flow stability and separation was clearly improved (Figure 11). These observations were also confirmed by the results from analysis with flow cytometry (Figure 17).

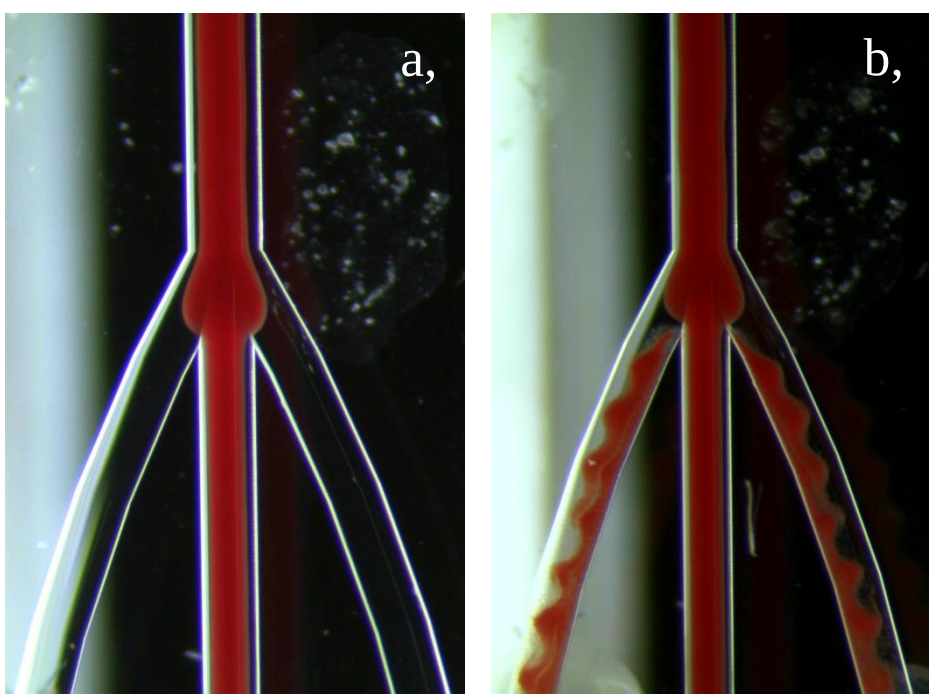

Figure 11: Whole blood separation (a) with pulsation damper and (b) without pulsation damper.

Results from separation with syringe pumps instead of peristaltic pumps was used as a point of reference when evaluating the performance and functionality of the

peristaltic pumps with pulsation dampers. RBC concentration in both outlets with different side outlet flow rates are shown for both pump types in Figure 12.

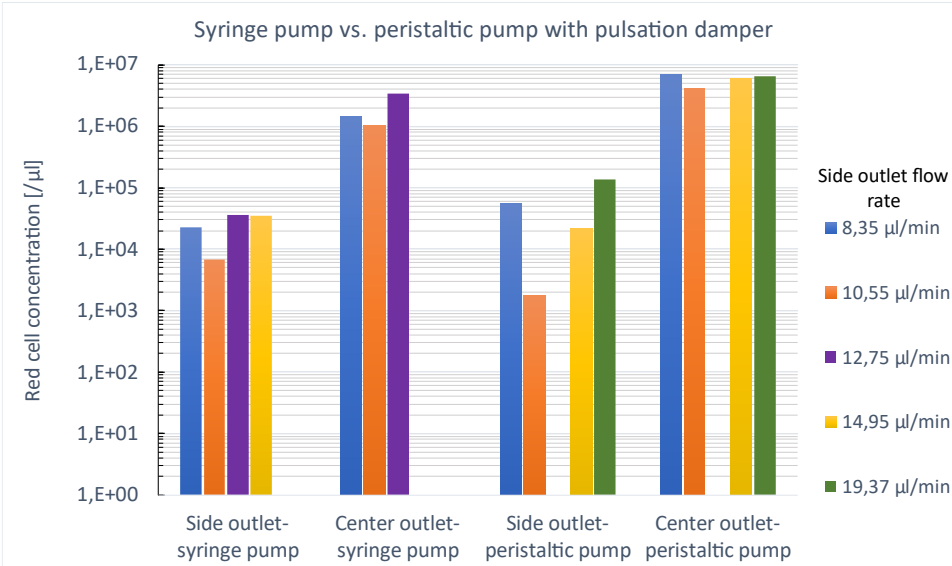

Figure 12: Comparison of separation with syringe pumps and peristaltic pumps. All separations were performed on the same day with whole blood from the same donor and each measure was performed only once. The measured red cell concentration also contains white blood cells, however, the fraction of white cells account for less than 1% of the total blood volume and therefore have minimal contribution to the measured concentration.

Syringe pumps were used at two different occasions for which the first attempt was only visually examined and not analyzed with flow cytometry. Figure 12 shows measurements from the second separation with syringe pumps next to measurements with peristaltic pumps in combination with pulsation dampers. The results indicate similar separation performance for both pump types. Worth to note is that the syringe pump measurements are not necessarily representative for the general performance of these pumps, as the first separation with syringe pumps was visually more stable than the second.

However, similar separation performance is also observed in Figure 13, showing an image from the first separation with syringe pumps next to an image of separation with peristaltic pumps.

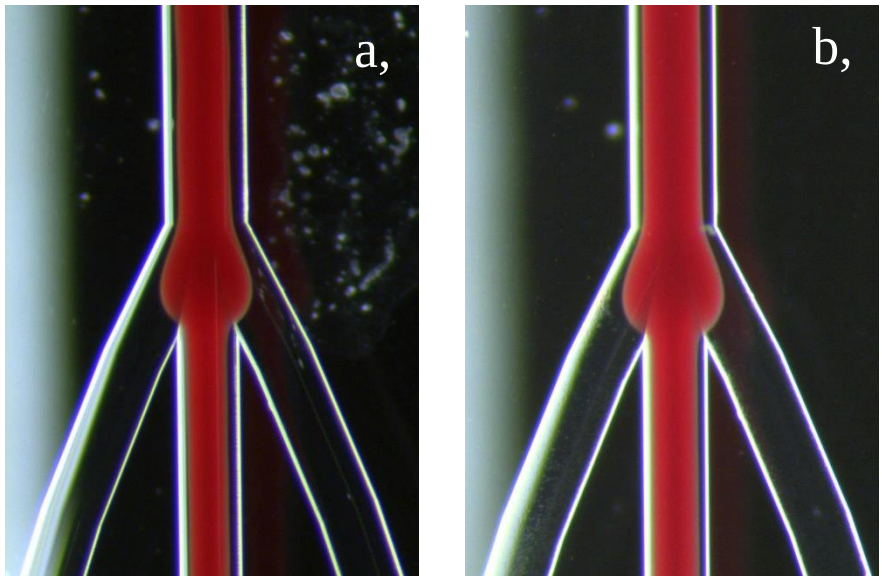

Figure 13: Separation when using (a) peristaltic pumps with pulsation dampers (b) syringe pumps at a side flow rate of 8 µl/min.

It is important to take into consideration that the pulsation dampers were built from materials available at hand without being specifically designed with the correct dimensions. The stabilizing effect of the damper is achieved by volume change of the air trapped in the damper which absorbs flow rate fluctuations. The trapped air is compressed during the phase with high pump flow rate which draws fluid into the damper. When the pump's flow rate decreases, the compressed air expands, pushing fluid out of the damper which compensates for the pump in the downstream flow rate.

There were times when the flow in the center of the channel was suddenly diverted into the side branches, resulting in red blood cells spilling over to the side outlet, Figure 14. The flow then quickly returned to a stable state again. The origin of these pulses is unknown, however, since they were not observed when syringe pumps were used, they are most likely derived from the pulse dampers or the peristaltic pumps. The pulses did not always occur during separation, which leads me to believe that they could be connected to formation of bubbles or movement of bubbles that affect the flow resistance of different flow paths. The pulses also occurred with varying frequency and amplitude, which should not have been the case if they were connected to the volume of the pulse dampers.

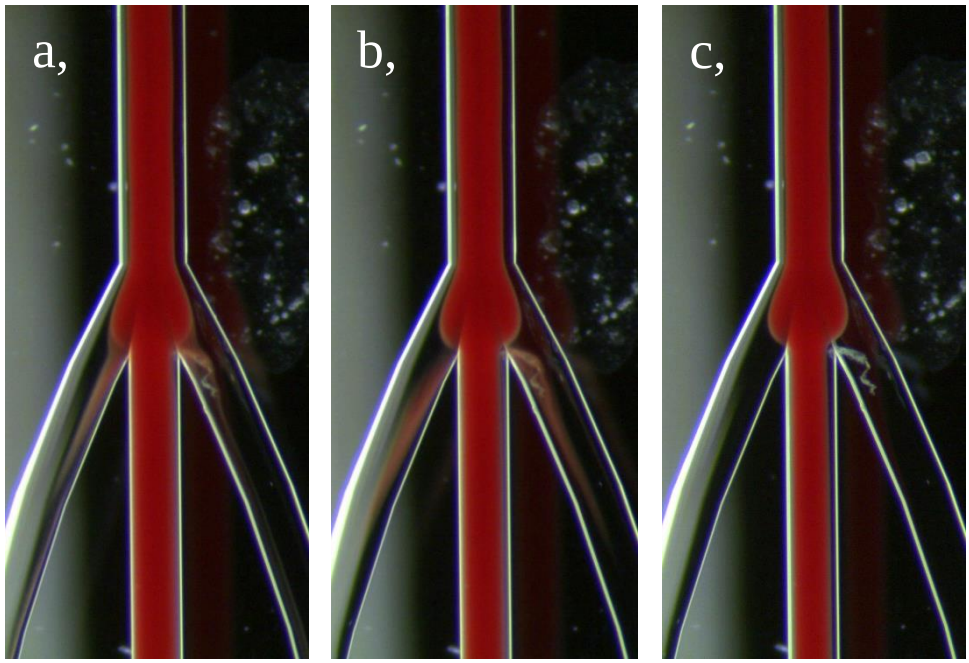

Figure 14: Low frequency pulse when using pulsation damper. (a) Pulse start, red cells are diverted to the side branches. (b) Direction of diverted flowlines are returned to the center outlet. (c) Flow returning to a stable state after the pulse ends.

The transition time from starting the pump until reaching a stable flow rate is affected by the introduction of a pulsation damper. Pressure is accumulated gradually by the air in the damper until reaching a stable pressure, after which the stabilizing effects occur. The time until the flow rate reaches zero after the pumps have been turned off is also increased. Flow rate downstream is decreased during the transition time, as part of the pressure that generates flow is instead accumulated in the damper.

Valves in the open ends of the system could have been added to prevent the flow delay when the pumps are stopped. The delay when starting the pumps would then also have been counteracted, however, pressure equilibrium would first need to be reached in the damper chamber. Which could then have been made with for example PBS before the pumps were stopped and the input fluid switched to whole blood.

The transition time is affected by the how much pressure that the damper can absorb for each pumping stroke and the volume of the damper gas. In the first homemade damper, a syringe was used to allow control of the volume of the damper chamber and the gas volume. Since the syringe piston was not fixed in position during separation, there is the possibility that the total volume of the

container could have change, however, no movement of the piston was visually observed. For the second homemade damper, the syringe was instead replaced with a plastic cap/plug, resulting in a section of fixed volume where gas could be trapped. Similar separation performance was visually observed for both damper versions. However, comparison of the two version might not be representative as the first damper was only used at two different flow rates while the second damp was tested using five different flow rates but only one or two times for each. The measured RBC concentration on the side outlet for each separation with the two damper versions is shown in Figure 15.

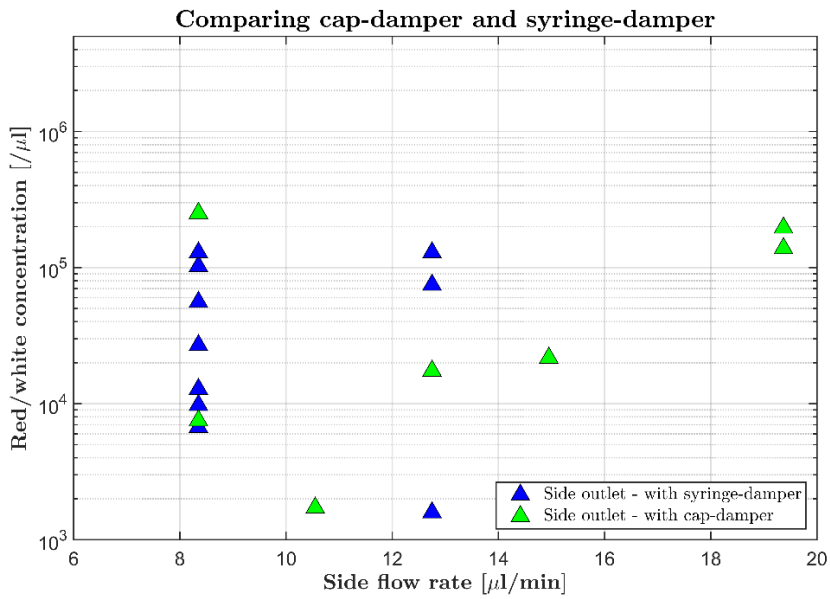

Figure 15: Red/white cell concentration different side flow rates in plasma separated using the two different types of home-made pulsation dampers.

With the volume of the second damper being much smaller than the first and both types showing similar stabilization performance, leads to the belief that they are not optimally sized. An undersized damper would not be able to adequately compensate for the pressure variation, while an oversized damper instead would store fluid and act as an accumulator. Accurate sizing of the damper is therefore important to achieve maximum stabilization of the flow. Distance between the damper and the pump also affect the dampening effect and should therefore be placed as close as possible to the pump discharge.

Further optimization of the damper size was not performed in this thesis. However, there are different ways for which this could have been done. One approach, described by the company Blacoh Fluid Control [44], is based on using the maximum and minimum pressure of the pump together with the pump

constant to calculate the optimal damper volume. Measurement of the pump pressure curve could have been performed to find the maximum and minimum pressure. To determine the pump constant (f_d) requires the pump pulse volume (V_p), which is approximately $0.389\ mm^3$ for the pumps used in this thesis. Gas filling (V_{fill}) of the damper is recommended to be between 80-90 %. Change of pressure in the damper is assumed to be an isentropic process and therefore calculated using equation (7), with n for air being 1.400. The following equations could then have been used to calculate the damper volume (V_d).

$$p_2 = \left(\frac{V_1}{V_2}\right)^n * p_1$$

$$V_1 = V_d * V_{fill}$$

$$V_2 = V_1 - V_p$$

$$f_d = \frac{V_1 * \left(1 - \left(\frac{p_1}{p_a}\right)^{\frac{1}{n}}\right)}{V_p} \tag{19}$$

in which p_a is the maximum absolute pressure and p_1 is the minimum absolute pressure. Equation (19) can then be rearranged to give V_d as

$$V_d = \frac{V_p * f_d * \left(\frac{p_2}{p_1}\right)^{\frac{1}{n}}}{V_{fill} * \left(\left(\frac{p_2}{p_1}\right)^{\frac{1}{n}} - 1\right)} \tag{20}$$

Most commercially available pulsation dampers operate based on the same stabilizing principle as the ones used in this project. However, a thin flexible membrane is often used to separate the damper gas from the fluid. As the gas compresses and decompresses, the membrane moves up and down, drawing and pushing fluid in and out of the damper. This way the gas cannot be dissolved in the liquid, otherwise slowly leading to decreased stabilizing ability by the damper.

4.1.5 Sampling loop

The concentration of RBCs in samples that were collected from the discharge of the side outlet pump were lower than what was expected from visually observing the separation. This observation can be explained by sedimentation of RBCs in

the tubes leading from the side outlet of the acoustic separator to the peristaltic pump. The pre-attached tubes have larger ID (0.8 mm) compared to the rest of the tubing which decreases flow rate and increases settling of RBCs in these tube segments.

An estimation of the sedimentation velocity using equation (11), for a red blood cell approximated as a sphere with radius 7.8 μm and density of $1125\ kg/m^3$ in plasma with density of $1025\ kg/m^3$ and viscosity 1.6 mPa/s, at room temperature, found the settling velocity to be $8.28\ \mu m/s$. The sedimentation time, $t_s = L/u_t$, for a length equal to the tube ID would then be $96.6\ s$.

At the lowest flow rate, $Q = 8.35\ \mu l/min$, it takes roughly $577.9\ s$ for RBCs to pass through the $16\ cm$ long pre-attached tube segment. Comparing the sedimentation time and passage time make it clear that a lot of RBCs will be settling at the bottom of the tube and measurement on the fluid at the discharge of the pump will yield an incorrect value on the separation efficiency.

To enable a more accurate measurement of the separation, a sampling loop was therefore built and placed between the separation chip and the peristaltic pump. This way, fluid is collected from a point closer to the point of separation and settling of RBC along the path of the flow is reduced.

Shown in Figure 16 is the RBC concentration in samples collected from the sampling loop and the discharge of the side outlet pump, both with and without pulsation dampers. This result confirms the observation of cells getting stuck in the system and that use of the sampling loop allows for a more accurate measure of the separation performance.

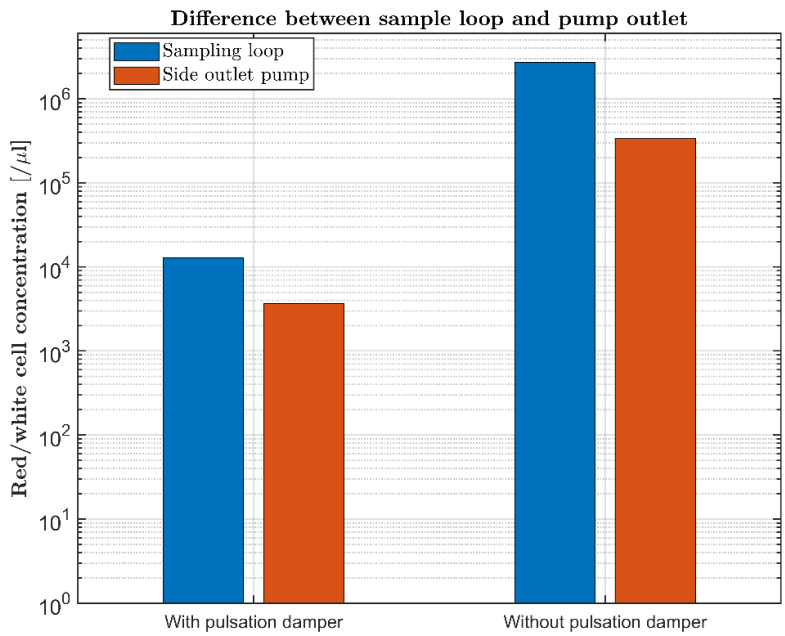

Figure 16: Red/white cell concentration in samples collected from the sample loop (blue) and the pump connected to the side outlet (red).

4.1.6 Analysis of flow cytometry data

The presented values on cell concentrations and separation performance were calculated using the flow cytometry data which is affected by the way the gates are placed. The strategy was to stain platelets and WBC and then identify which populations they were found in on a FSC vs SSC plot based on the detected fluorescence signal. Knowing the different cell types found in whole blood, their relative size, and occurrence, it is reasonable to assume that the placed gate correctly includes both RBC and WBCs.

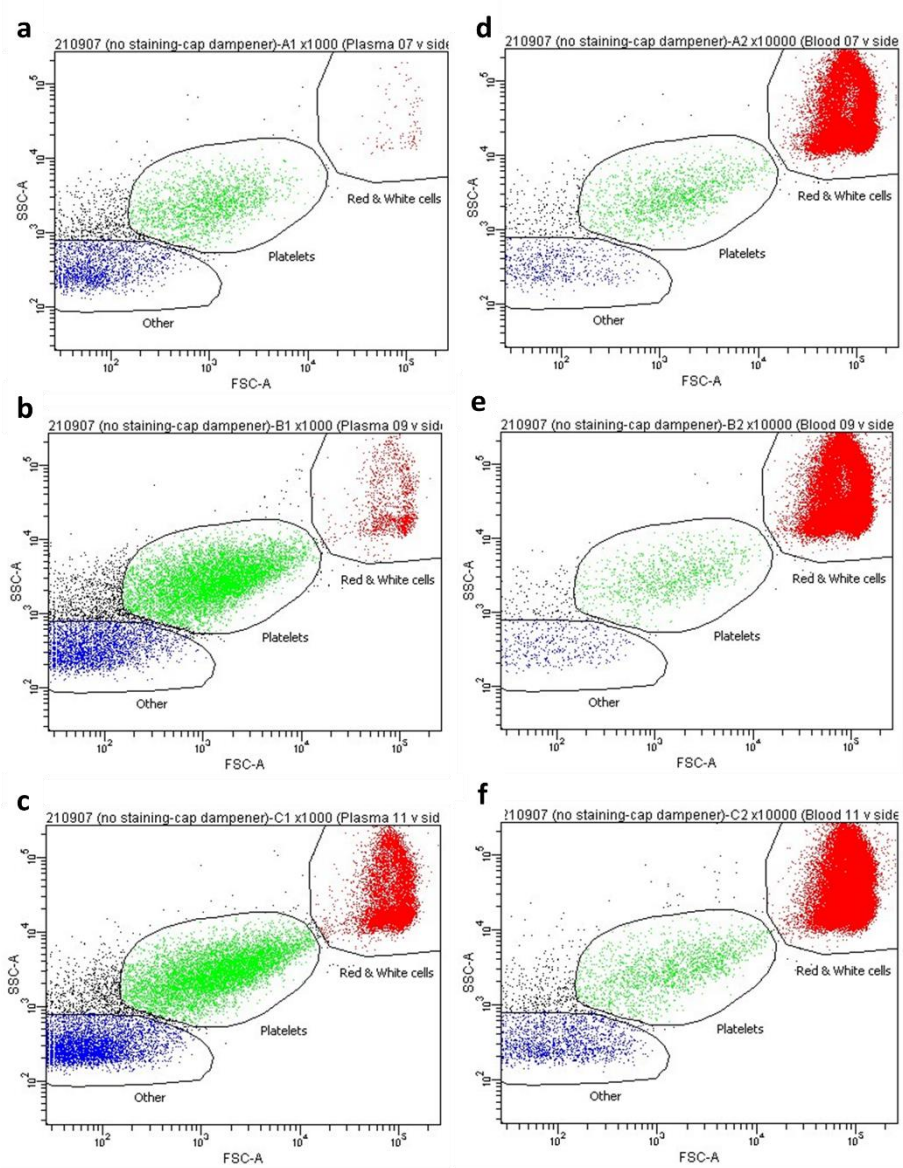

*Figure 17: Flow cytometry data in three different samples collected from side outlet (**a-c**) and center outlet (**d-f**) when using pulsation dampers. The flow rate in center outlet was 58 µl/min and the flow rate in side outlet was (**a, d**) 10.55 µl/min (**b,e**) 14.95 µl/min (**c, f**) 19.36 µl/min.*

FSC vs SSC data from flow cytometry analysis of samples separated when pulsation dampers were applied are shown in Figure 17. The population with red blood cells is clearly visible in data from the center outlet, Figure 17 (d-f). For the lowest side flow rate (10.55 µl/min), however, this population is reduced to only a handful of red blood cells, Figure 17 (a). As expected, the red blood cell population in the side outlet fraction grows as the side flow rate increases.

4.2 Separation and function

4.2.1 Separation with polystyrene beads

This section includes the results from separation of PS beads suspended in MilliQ. The pump configurations described in Figure 3 were tested with different flow rates to see how various outlet flow ratios affected the separation. Both 5- and 7-µm-PS beads were used and optimally focused to the center of the separation channel when the piezoceramic transducer operated at a frequency of either 1.959 MHz or 2.033 MHz.

Pump configuration C, with peristaltic pumps on both outlets, had the best separation performance. The effect on separation from pulsations generated by the peristaltic pumps was clearly visible, shown in Figure 18 by two consecutive frames from separation with PS beads.

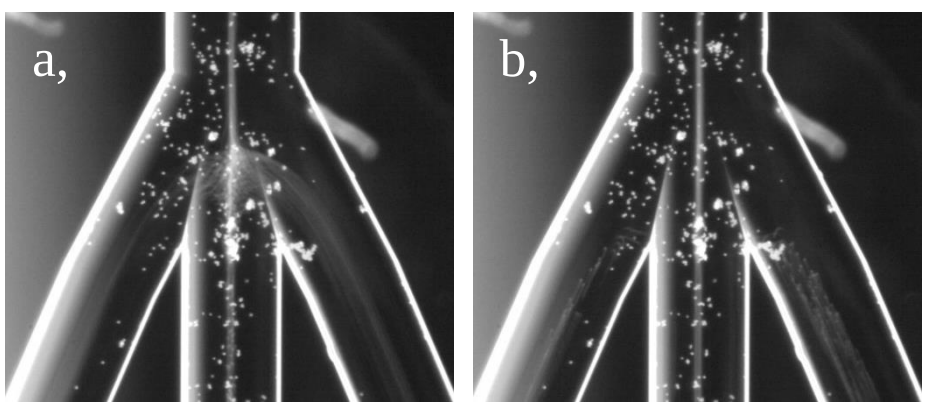

Figure 18: Pulsation generated by the peristaltic pumps. (a) Start of a new pulsation, beads are directed from the center of the channel into the side branches. (b) End of the pulsation, beads stay in the center and follow the flow into the center outlet.

4.2.2 Separation with whole blood

For separation to be successful, the red blood cells need to be focused into a narrow band at the center of the separation channel. The first separation with whole blood was performed to find out which actuation frequency to use and how large of an acoustic energy was needed to focus the cells. Frequencies around 2 MHz were examined visually, and the best focus was found at 2,042 MHz.

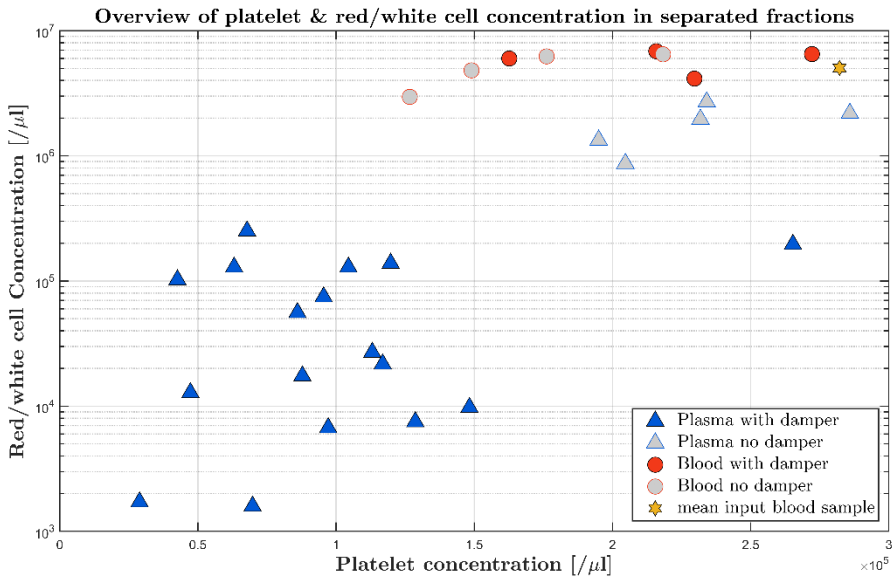

Figure 19: Overview of separated blood fractions.

Figure 19 shows that the concentration of RBCs in the side outlet on average was reduced by a factor of about 100 when applying the pulsation dampers. The spread of the RBC concentration in the group from the side outlet with attenuator also varies by about a factor of 100. This can be partly explained by the fact that different flow rates were used for the different samples, which is not shown here. The long collection time may also have contributed to the spread as both sedimentation of RBCs in the input blood sample and the risk of bubbles forming increase over time. The whole blood sample was stirred using a tube and a syringe to avoid sedimentation. However, the stirring was not always done at the same time intervals, which may have affected the result.

The primary acoustic radiation force increases with cell size, which is why the center of the separation channel is mainly occupied by RBCs when the ultrasound is turned on. The platelets should be pushed out from the centre as the force acting one of them is smaller. Still, there is a trend that platelets exit the acoustic separator through the centre outlet. Movement of the platelets towards the center of the channel could also be affected by acoustic streaming.

The underlying mechanism involved in acoustic separation of dense suspensions is described by Karthick and Sen [43, 45] as an interplay between acoustic and shear induced diffusion forces. The primary acoustic radiation force is mainly responsible for RBC migration towards the center of the channel while SID force acts in the opposite direction and counteract focusing of the cells. Focusing of cells by the acoustic force increases cell concentration in the center of the channel, leading to an increased shear rate and SID force. For a given HCT and

flow rate, there exists a critical acoustic energy density above which cells are focused in the center and cell-free plasma forms by the walls. The focused width of cells will decrease asymptotically towards a minimum possible focusing width with increasing acoustic energy density. The authors describe the interplay between the two forces based on timescales for each effect and presents a theoretical model that can be used to predict the width of the focused cells in terms of shear rate, acoustic energy density, and cell concentration[45]. They also present an acoustofluidic device for blood plasma separation[43] with improved design based on the design by Lenshof et al.[7].

The pump connected to the center outlet was operating at 58 µl/min for all separation attempts, while the side outlet flow rate was varied to measure how the flow ratio affected separation. That the center outlet flow was kept constant and not the inlet flow might have been a mistake in retrospect. A better study of how the flow rate affects the separation would have been possible if the inlet flow had been kept constant instead. Increasing side flow rate would not only affect the width of the fluid flowing towards each outlet, but it also affects the total time the cells are affected by the primary acoustic radiation force and therefore also migration towards the channel center.

Measured RBC concentration in the side outlet with and without pulsation dampers are shown in Figure 20. The hypothesis was that below a certain flow rate, there would be very few red cells in the side outlet as the width of the focused RBCs would be very narrow. Above this flow threshold, the measured RBC concentration was expected to increase with increasing flow rate as the width of the RBCs grows.

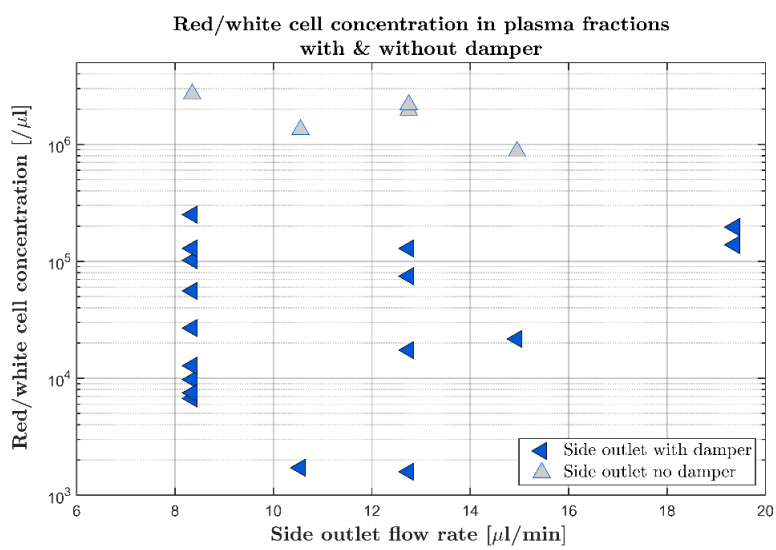

Figure 20: Comparison of red/white cell concentration in plasma using different side flow rates with and without a pulsation damper.

Looking at the group where no pulsation damper was used, separation does not agree with the expected behavior. This is most likely due to the pulsatile flow generated by the peristaltic micropumps. The relation almost seems to be reversed, with the RBC concentration instead decreasing with increasing flow rate. This could be related to the flow being less pulsatile when operating the pumps at higher rpm. For the group with pulsation dampers, most of the samples were separated using the lowest flow rate settings, which show a large spread in RBC concentration. A trend corresponding to the expected behavior can be seen provided that the lowest flow rate measurements are excluded.

Measured platelet concentration in the side outlet with and without pulsation dampers are shown in Figure 21. The results for the group without pulsation damper is similar independently of flow rate. For the other group, with pulsation damper, there trend is increasing with increasing flow rate, provided that the data using the lowest flow rate is excluded. One thing worth mentioning, is that $7/9$ of the samples at the lowest flow rate used the first type of pulsation damper, as seen in Figure 15.

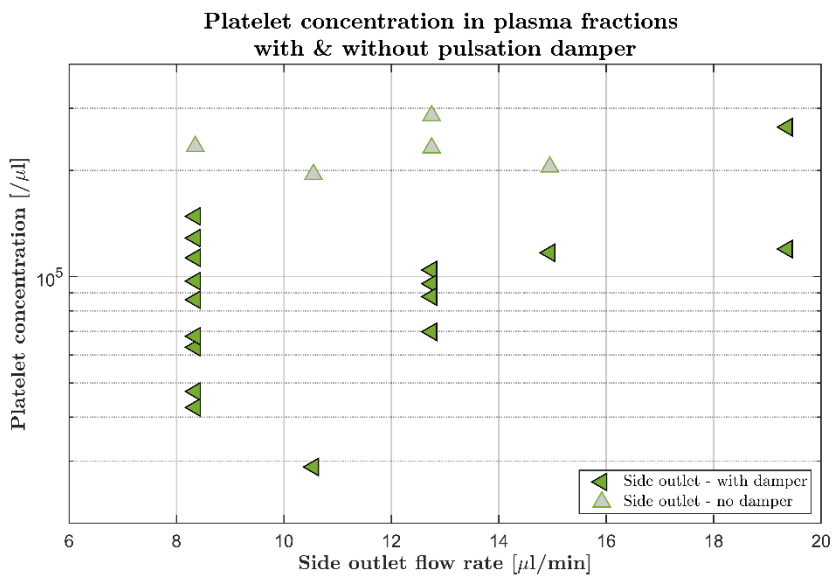

Figure 21:Comparison of platelet concentration in plasma using different side flow rates with and without pulsation damper.

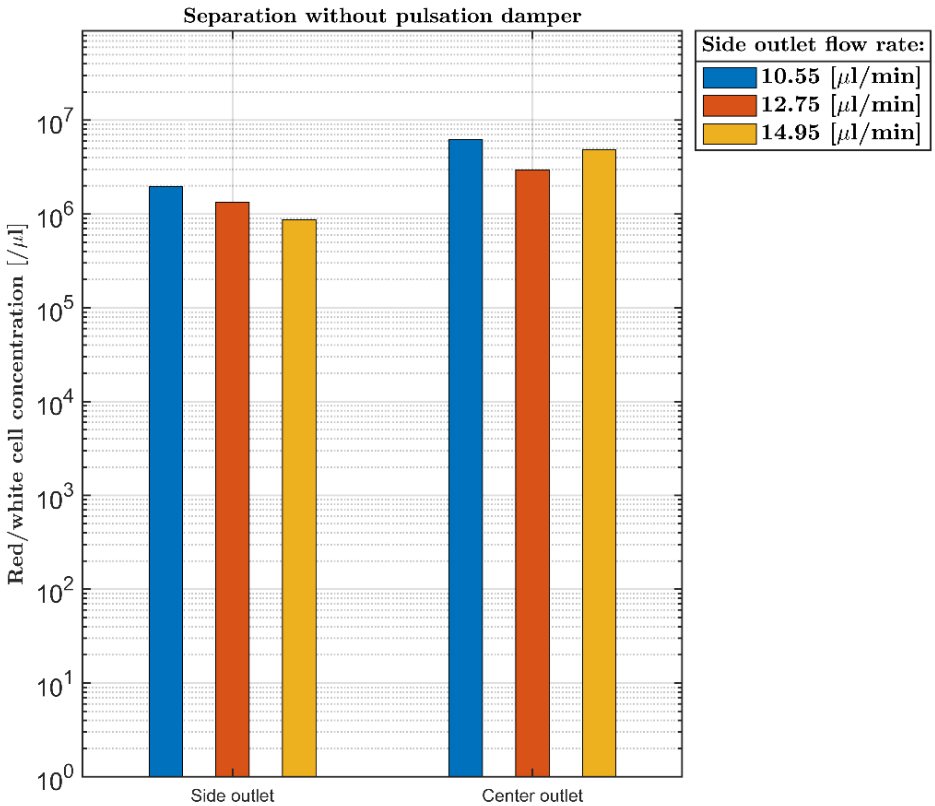

Figure 22: Red/white cell concentration in both outlets from separation with pulsation damper using different flow rates for each pair. The same whole blood sample was used for all three pairs.

RBC concentration in both the outlets from separation without pulsation damper at three different flow rates using the same whole blood sample is shown in Figure 22. Concentration is only slightly reduced in the side outlet compared to the center outlet. As previously described for separation without pulsation damper, the separation does not seem to be corresponding to the expected behavior.

Figure 23 shows the RBC concentration in the whole blood sample and in both separated fraction at different flow rates. A clear improvement is observed in the reduction of RBCs compared to when dampers were not used. Concentration also increases with increased side flow rate as is expected as the flow closer to the channel center are diverted to the side outlet when flow ratio is increased. The total flow rate in the separation channel also increases, which leads to cells spending a shorter time in the separation channel and are less affected by the primary acoustic radiation force.

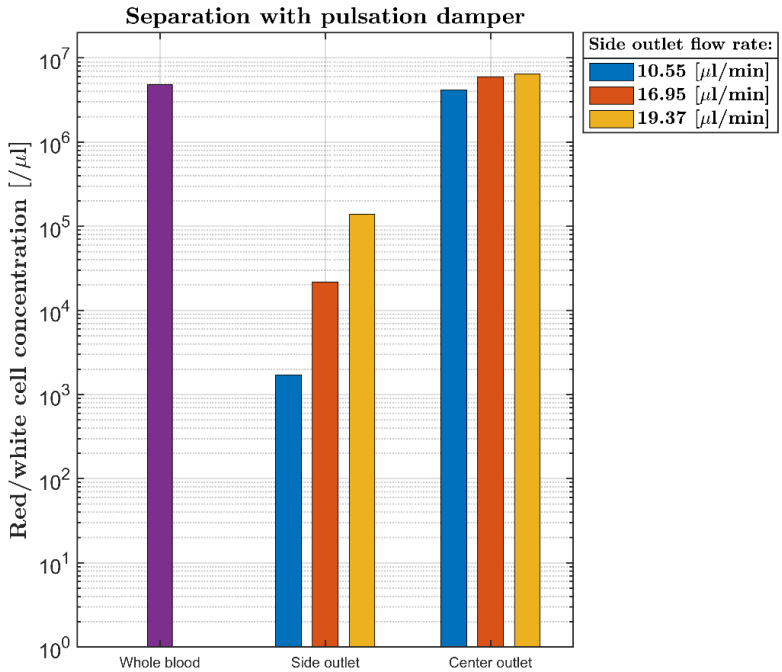

Figure 23: Red/white cell concentration in both outlets from separation with pulsation damper using different flow rates for each pair. Concentration of the whole blood sample that was used for all three pairs is also included.

4.2.3 Acoustic separation with fetal blood

Extraction of blood plasma from fetal blood was never tested with the experimental setup. The high concentration of RBCs found in preterm blood would lead to a wider focusing width of cells that likely would result in contamination of RBCs in the plasma fraction. Separation of blood with higher HCT could have been tested by removal of plasma from whole blood after centrifugation.

Acoustophoresis-based separation chips have been reported in which the initial RBCs concentration is reduced along the separation channel through multiple extraction outlets, located in the center of the channel [7, 18, 43]. An acoustic separation chip with similar design could potentially be used to solve the problem with high HCT and plasma extraction with fetal blood.

Chapter 5

Conclusion

The main aim for this project was to investigate if peristaltic pumps could be used for acoustophoresis based blood plasma separation with whole blood. For which the application of intended use is the development of miniaturized diagnostic POC devices that minimize loss of endogenous blood components by directly returning part of the separated blood to the patient. The results from separation with the experimental setup suggest that peristaltic pumps could be used to achieve separation equivalent to when syringe pumps are used.

In conclusion, peristaltic pumps were used in an experimental setup to separate blood plasma from whole blood by acoustophoresis. The results indicated that the fundamental design of the experimental setup and functionality of the peristaltic pumps when combined with pulsation dampers are promising

It remains to be investigated whether acoustophoresis can be used to extract blood plasma from fetal blood while returning enriched blood. However, the use of peristaltic pumps opens for new possibilities to develop closed microfluidic systems with a reduced risk of blood contamination.

References

1. Norman M, Hallberg B, Abrahamsson T, Björklund LJ, Domellöf M, Farooqi A, et al. Association Between Year of Birth and 1-Year Survival Among Extremely Preterm Infants in Sweden During 2004-2007 and 2014-2016. JAMA. 2019;321(12):1188-99.

2. Challis P, Nydert P, Håkansson S, Norman M. Association of Adherence to Surfactant Best Practice Uses With Clinical Outcomes Among Neonates in Sweden. JAMA Netw Open. 2021;5(4):e217269.

3. One-Year Survival of Extremely Preterm Infants After Active Perinatal Care in Sweden. JAMA. 2009;301(21):2225-33.

4. Hellström W, Forssell L, Morsing E, Sävman K, Ley D. Neonatal clinical blood sampling led to major blood loss and was associated with bronchopulmonary dysplasia. Acta Paediatr. 2020;109(4).

5. Jobe AH, Ikegami M. Pathophysiology of Respiratory Distress Syndrome and Surfactant Metabolism. Fetal and Neonatal Physiology. Philadelphia: W.B. Saunders; 2011. p. 1137-50.

6. Schwarz KB, Dear PRF, Gill AB, Newell SJ, Richards M. EFFECTS OF TRANSFUSION IN ANEMIA OF PREMATURITY. Pediatric Hematology and Oncology. 2005;22(7):551-9.

7. lenshof A, Ahmad Tajudin A, Järås K, Swärd-Nilsson AM, Aberg L, Marko-Varga G, et al. Acoustic Whole Blood Plasmapheresis Chip for Prostate Specific Antigen Microarray Diagnostics. Analytical Chemistry. 2009;81(15):6030-7.

8. Widness JA. Pathophysiology of Anemia During the Neonatal Period, Including Anemia of Prematurity. NeoReviews. 2008;9(11):e520.

9. Saito-Benz M, Flanagan P, Berry MJ. Management of anaemia in pre-term infants. British journal of haematology. 2020;188(3):354-66.

10. Carroll PD, Widness JA. Nonpharmacological, Blood Conservation Techniques for Preventing Neonatal Anemia—Effective and Promising Strategies for Reducing Transfusion. Seminars in Perinatology. 2012;36(4):232-423.

11. hellström W, Martinsson T, Hellström A, Morsing E, Ley D. Fetal haemoglobin and bronchopulmonary dysplasia in neonates: an observational study. Archives of disease in childhood Fetal and neonatal edition. 2021;106(1):88-92.

12. Madsen LP, Rasmussen MK, Bjerregaard LL, Nohr SB, Ebbesen F. Impact of blood sampling in very preterm infants. Scandinavian Journal of Clinical and. 2000;60(2):125-32.

13. Obladen M, Sachsenweger M, Stahnke M. Blood sampling in very low birth weight infants receiving different levels of intensive care. European Journal of Pediatrics. 1988;147:399-404.

14. Hellström W, Martinsson T, Morsing E, Gränse L, Ley D, Hellström A. Low fraction of fetal haemoglobin is associated with retinopathy of prematurity in the very preterm infant. 2021.

15. Madan A, Kumar R, Adams MM, Benitz WE, Geaghan SM, Widness JA. Reduction in Red Blood Cell Transfusions Using a Bedside Analyzer in Extremely Low Birth Weight Infants. Journal of Perinatology. 2005;25(1):21-5.

16. Sengupta P, Khanra K, Chowdhury AR, Datta P. 4 - Lab-on-a-chip sensing devices for biomedical applications. From Materials to Devices - Fabrication, Applications and Reliability: Woodhead Publishing Series in Electronic and Optical Materials; 2019. p. 47-95.

17. Nikoleli G-P, Siontorou CG, Nikolelis DP, Bratakou S, Karapetis S, Tzamtzis N. Chapter 13 - Biosensors Based on Microfluidic Devices Lab-on-a-Chip and Microfluidic Technology. Nanotechnology and Biosensors: Elsevier; 2018. p. 375-94.

18. Ahmad Tajudin A, Petersson K, Lenshof A, Swärd-Nilsson AM, Ånerg L, Marko-Varga G, et al. Integrated acoustic immunoaffinity-capture (IAI) platform for detection of PSA from whole blood. Lab on a chip. 2013;13(9):1790-6.

19. Mielczarek WS, Obaje EA, Bachmann TT, Kersaudy-Kerhoas M. Microfluidic blood plasma separation for medical diagnostics: is it worth it? Lab Chip. 2016;16(18):3441-8.

20. Barbosa AI, Reis NM. A critical insight into the development pipeline of microfluidic immunoassay devices for the sensitive quantitation of protein biomarkers at the point of care. Analyst. 2017;142(6):858-82.

21. Platelet [Internet]. Encyclopedia Britannica. 2008 [cited 2021-10-07]. Available from: https://www.britannica.com/science/platelet.

22. Red blood cell [Internet]. Encyclopedia Britannica. 2020 [cited 2021-10-07]. Available from: https://www.britannica.com/science/red-blood-cell.

23. Fernandez Arias C, Fernandez Arias C. How do red blood cells know when to die? Royal Society open science. 2017;4(4).

24. MedlinePlus [Internet]. 2020 [cited 2021-09-26]. Available from: https://medlineplus.gov/ency/article/003648.htm.

25. Jopling J, Henry E, Wiedmeier SE, Christensen RD. Reference ranges for hematocrit and blood hemoglobin concentration during the neonatal period: data from a multihospital health care system. Pediatrics. 2009;123(2):e333-e7.

26. White blood cell [Internet]. Encyclopedia Britannica. 2021 [cited 2021-09-30]. Available from: https://www.britannica.com/science/white-blood-cell.

27. Handin RI, Lux SE, Stossel TP. Life cycle of mononuclear phagocytes. Blood: Principles and Practice of Hematology. 1. Philadelphia: Lippincott Williams & Wilkins; 2003. p. 471.

28. Swanepoel AC, Stander A, Pretorius E. Flow cytometric comparison of platelets from a whole blood and finger-prick sample: impact of 24 hours storage. Hematology. 2013;18(2):106-14.

29. Plasma [Internet]. Encyclopedia Britannica. 2020 [cited 2021-10-08]. Available from: https://www.britannica.com/science/plasma-biology.

30. Guzzetta NA. Benefits and risks of red blood cell transfusion in pediatric patients undergoing cardiac surgery. Pediatric Anesthesia. 2011;21:504-11.

31. SHARMA S, SHARMA P, TYLER LN. Transfusion of Blood and Blood Products: Indications and Complications. Am Fam Physician. 2011;83(6):719-24.

32. Castillo B, Dasgupta A, Klein K, Hlaing T, Wahed A. Chapter 7 - Blood components: Transfusion practices. Transfusion Medicine for Pathologists: Elsevier Inc; 2018. p. 125-42.

33. Ong S-E, Zhang S, Fu Y. Fundamental principles and applications of microfluidic systems. Frontiers in Bioscience. 2008;13:2757-61.

34. Dey S, Zeeshan Ali S, Padhi E. Terminal fall velocity: the legacy of Stokes from the perspective of fluvial hydraulics. Proceedings of the Royal Society A: Mathematical, Physical and Engineering Sciences. 2019;475(2228):20190277.

35. Bruus H. Acoustofluidics 7: The acoustic radiation force on small particles. Lab on a Chip. 2012;12(6):1014-21.

36. Bruus H. Acoustofluidics 1: Governing equations in microfluidics. Lab on a Chip. 2011;11(22):3742-51.

37. Antfolk M, Laurell T. Acoustofluidic Blood Component Sample Preparation and Processing in Medical Applications. Applications of

Microfluidic Systems in Biology and Medicine. Singapore: Springer Singapore; 2019. p. 1-25.

38. Rusconi R, Stone HA. Shear-Induced Diffusion of Platelike Particles in Microchannels. Physical Review Letters. 2008;101(25):254502.

39. McKinnon KM. Flow Cytometry: An Overview. Current protocols in immunology. 2018;120:5.1.-5.1.11.

40. Schmit T, Klomp M, Khan NM. An Overview of Flow Cytometry: Its Principles and Applications in Allergic Disease Research. Animal Models of Allergic Disease: Methods and Protocols. New York, NY: Springer US; 2021. p. 169-82.

41. Rensheng Deng YC, Chi-Hwa Wang,. Experiments and simulation on a pulse dampener system for stabilizing liquid flow. Chemical Engineering Journal. 2012;210(1):136-42.

42. Helms CC, Marvel M, Zhao W, Stahnke M, Vest R, Kato GJ, et al. Mechanisms of hemolysis-associated platelet activation. Journal of Thrombosis and Haemostasis. 2013(11):2148-54.

43. Karthick S, Sen AK. Improved Understanding of Acoustophoresis and Development of an Acoustofluidic Device for Blood Plasma Separation. American Physical Society. 2018;10(3):034037.

44. McComb D. Sizing Pulsation Dampeners Is Critical to Effectiveness [Available from: https://www.blacoh.com/downloads/literature/Sizing_Pulsation_Dampeners_Is_Critical_to_Effectiveness_P47E11_010.pdf.

45. Karthick S, Sen AK. Role of shear induced diffusion in acoustophoretic focusing of dense suspensions. Applied Physics Letters. 2016;109(1):014101.